

**Wet-runway overruns: still a slippery problem**

*John O'Callaghan*

*National Resource Specialist – Aircraft Performance  
National Transportation Safety Board (NTSB), U.S.A.*

*ISASI #61728148*

## Table of Contents

Abstract .....	1
Introduction .....	2
Calculating the $\mu_B$ achieved during a landing ground roll.....	4
Physical parameters affecting $\mu_B$ on a wet runway: ESDU models, old & new .....	6
Hydroplaning on wet runways.....	15
Estimating the depth of water on wet runways.....	16
Modeling $\mu_B$ in the TALPA and GRF frameworks .....	18
Wet-runway $\mu_B$ defined in 14 CFR 25.109.....	22
NASA $\mu_B$ model based on Continuous Friction Measurement Equipment (CFME) data .....	24
Combined NASA and §25.109(c) $\mu_B$ model .....	26
Comparisons of actual and modeled $\mu_B$ .....	27
Estimating the ESDU 05011 F1 value from CFME data.....	31
Guidance concerning braking performance on wet runways: SAFOs 15009 and 19003.....	34
Flight Test Harmonization Working Group wet runway regulatory recommendations.....	36
Rainfall rate descriptors in surface weather observations and reports.....	37
Summary and conclusions .....	38
Acknowledgements .....	40
References .....	40
Glossary.....	41
Endnotes .....	43

## **Wet-runway overruns: still a slippery problem**

***John O'Callaghan***

*National Resource Specialist – Aircraft Performance  
National Transportation Safety Board (NTSB), U.S.A.  
ISASI #61728148*

### **Abstract**

Over the past fifteen years, the NTSB has led or participated in the investigation of a number of runway overrun accidents and incidents that occurred after the airplanes involved landed on wet runways. An analysis of the airplane stopping performance during these events indicates that in most cases, the wheel braking friction coefficient ( $\mu_B$ ) achieved during the landing roll was significantly less than both the  $\mu_B$  assumed in the wet-runway landing distance advisory data provided in the manufacturers' Airplane Flight Manuals (AFMs), and the wet-runway  $\mu_B$  specified in the Runway Condition Assessment Matrix (RCAM) advanced by the U.S.A. Federal Aviation Administration (FAA) through the Takeoff And Landing Performance Assessment (TALPA) framework, and by the International Civil Aviation Organization (ICAO) through the Global Reporting Format (GRF) framework. In recognition of this problem, the FAA has issued a safety alert to operators warning them that the advisory data for wet runway landings may not provide a safe stopping margin under all conditions. In addition, an Aviation Rulemaking Advisory Committee (ARAC) has recommended adding new requirements to the U.S.A. 14 *Code of Federal Regulations* (CFR) Part 25 transport category airplane certification standards and to the Part 121 air-carrier dispatch rules to account for potential shortfalls in  $\mu_B$  in wet conditions. This paper reviews the physics underlying wet-runway stopping performance and the factors affecting  $\mu_B$ , and compares the  $\mu_B$  achieved in several overrun events with the  $\mu_B$  predicted by several models (including the RCAM). The results indicate that the new certification and dispatch requirements proposed by the ARAC have merit, and that the additional conservatism in these proposals could benefit the operators of all turbine-powered airplanes, not just air-carriers operating Part 25 transport-category airplanes. The results also indicate that, in extreme rainfall conditions, even this additional conservatism cannot compensate for the potential reduction in  $\mu_B$ , and that landings in these conditions are best avoided. Prudently avoiding landings in dangerous rainfall conditions without unnecessarily disrupting operations will require identifying and communicating the presence of such conditions to flight crews. This in turn will likely require new rainfall rate descriptors that identify rainfall rates that can be several multiples of the current "heavy" rain threshold, and updating the RCAM to incorporate these descriptors.

## Introduction

A “landing overrun” accident is one in which an airplane, following touchdown on a runway, fails to stop on the paved surface and travels past (“overruns”) the end of the runway, resulting in sufficient damage or injury to legally qualify as an “accident.” According to the NTSB accident database, between January 1, 2008 and May 11, 2023, landing overruns accounted for 57 of 652 accidents (8.7%) investigated by the agency involving turbine-powered airplanes (see Table 1). Of these, 10 were on wet runways, 8 were on runways contaminated with frozen precipitation, and in the rest (39) the runway condition was not listed as a contributing factor. Two of these 39 involved at least one fatality.<sup>1</sup> Internationally, an ICAO “SkyTalks” presentation on the GRF identified “runway safety” as a global safety priority (along with controlled-flight-into-terrain and loss-of-control), and noted that “runway excursions” are the “highest [runway safety] risk category.”<sup>2</sup>

While operational errors, such as higher than nominal airspeed or tailwind components, long touchdown distances, and delayed use of deceleration devices (such as spoilers, reverse thrust, and brakes) are often contributing factors to landing overruns, less-than-expected runway friction is also a common contributing factor in landing overruns on runways that are not dry. A “non-dry” runway is one that is either wet, flooded, or “contaminated” with frozen precipitation (any combination of slush, snow, or ice).<sup>3</sup> For most turbine-powered airplane operations, the increased landing distance required to land on a non-dry runway are specified in operational regulations as safety factors applied (at the time of dispatch) to the required dry-runway landing distance. However, following a fatal landing overrun in 2005, the United States Federal Aviation Administration (FAA) began developing standardized procedures by which operators could compute required landing distances on non-dry runways accounting for actual runway conditions at arrival (and consequent reduced runway friction). The results of this development are implemented today in the TALPA framework used in the U.S.A., and the GRF framework advanced by ICAO. The foundation of both frameworks is the Runway Condition Assessment Matrix (RCAM), which provides a consistent method for assessing and describing runway surface conditions, and for modeling the associated friction level of the runway. As of October 2016, federally-obligated airports in the U.S.A. report runway conditions using the RCAM, though the use of the RCAM and associated TALPA guidance by operators to compute required landing distances remains voluntary. The ICAO GRF framework became applicable worldwide in November 2021.

Ref. 1, published in 2016, describes how an analysis of several wet-runway landing overruns investigated by the NTSB indicates that the wheel braking friction coefficient ( $\mu_B$ ) achieved during each landing roll was significantly less than the  $\mu_B$  predicted by industry-accepted models (including the RCAM), and less than the  $\mu_B$  assumed in the wet-runway landing distance advisory data provided in the manufacturers’ AFMs. This paper updates the findings of Ref. 1 with two additional wet-runway overrun cases, and examines how extreme rainfall rates can reduce  $\mu_B$  to a level significantly below that modeled in the RCAM. The new 14 CFR Part 25 and Part 121 regulations proposed by the ARAC are also presented, and shown to have merit considering the actual  $\mu_B$  attained in the overrun accidents described .

Item	NTSB database, 01/01/2008 – 05/11/2023	
Total accidents (fixed-wing, turbine)	652	
Total landing accidents	162	24.8% of all accidents
All landing runway overruns	57	35.2% of total landing accidents
Wet or flooded overruns (H <sub>2</sub> O)	10	17.5% of overruns (6.2% of total landing accidents)
Frozen contaminants overruns	8	14.0% of overruns (4.9% of total landing accidents)

## (a) Non-fatal accidents

Item	NTSB database, 01/01/2008 – 05/11/2023	
Total fatal accidents	77	11.8% of all accidents
Total fatal landing accidents	6	7.8% of all fatal accidents
Fatal landing runway overruns	2	33.3% of total fatal landing accidents
Fatal wet or flooded overruns (H <sub>2</sub> O)	0	0% of fatal overruns
Fatal frozen contaminants overruns	0	0% of fatal overruns

## (b) Fatal accidents

**Definitions:**

NTSB database: Includes U.S. Civil Aviation only (U.S. registered aircraft, anywhere in the world).

Total accidents = accidents investigated by the NTSB involving a fixed-wing aircraft with either turbofan, geared turbofan, or turbojet engine.

Total landing accidents = accidents investigated by the NTSB involving a fixed-wing aircraft with either turbofan, geared turbofan, or turbojet engine, where the phase of flight was either landing, landing-aborted after touchdown, landing-flare / touchdown, or landing-landing roll.

All landing runway overruns = accidents investigated by the NTSB involving a fixed-wing aircraft with either turbofan, geared turbofan, or turbojet engine; the defining event of the accident was either runway excursion or loss of control on ground; and the phase of flight was either landing, landing-aborted after touchdown, landing-flare / touchdown, or landing-landing roll.

Wet or flooded overruns (H<sub>2</sub>O) = accidents from the “all landing runway overruns” set where “environmental issues / physical environment / runway, landing, surface, wet surface” was cited as either causal to the accident or a contributing factor.

Frozen contaminants overruns = accidents from the “all landing runway overruns” set where “environmental issues / physical environment / runway, landing, surface, snow / slush / ice covered surface” was cited as either causal to the accident or a contributing factor.

Total fatal accidents = accidents from the “all accidents” set that involved at least one fatality.

Total fatal landing accidents = accidents from the “total landing accidents” set that involved at least one fatality.

Fatal landing runway overruns = accidents from the “total fatal landing accidents” set where the defining event of the accident was either runway excursion or loss of control on the ground.

Fatal wet or flooded overruns (H<sub>2</sub>O) = accidents from the “total fatal landing accidents” set where “environmental issues / physical environment / runway, landing, surface, wet surface” was cited as either causal to the accident or a contributing factor.

Fatal frozen contaminants overruns = accidents from the “total fatal landing accidents” set where “environmental issues / physical environment / runway, landing, surface, snow / slush / ice covered surface” was cited as either causal to the accident or a contributing factor.

**Table 1.** Summary of landing overrun statistics in the NTSB database between 01/01/2008 and 05/11/2023.

Note that both Ref. 1 and this paper only consider the  $\mu_B$  reduction on *wet* runways. Runways contaminated with frozen precipitation (“icy” runways) are not considered here. In some ways, wet runways can be as challenging as icy runways. Per Table 1, there are slightly more wet-runway overruns in the NTSB database than icy-runway overruns. Further, a sudden storm or shower can quickly make a dry runway very wet, and so make it harder for operators to anticipate and prepare for landings on wet runways that they expected to be dry.

Mirroring Ref. 1, the sections that follow review the physics underlying an airplane’s stopping performance and the factors that affect  $\mu_B$  on a wet runway, and describe a method for computing  $\mu_B$  from recorded data. The  $\mu_B$  models underlying the RCAM are also presented, and compared with the  $\mu_B$  observed in several wet runway landing overruns, and with  $\mu_B$  models based both on ground vehicle (Continuous Friction Measuring Equipment (CFME)) friction measurements and on theoretical formulations. As will be seen, the RCAM  $\mu_B$  models currently in use consistently overestimate the  $\mu_B$  that is actually achieved in wet-runway overruns, while  $\mu_B$  estimates based on CME devices better match the attained  $\mu_B$  (particularly when the CFME  $\mu_B$  is modified to account for higher water depths using theoretical considerations). Consequently, there is merit in accounting for lower  $\mu_B$  values than those modeled in the RCAM, as proposed in the new certification and dispatch requirements advanced by the ARAC. In addition, the most severe rainfall rate descriptor available (“heavy” rain) fails to identify rainfall rates that can be several multiples of the “heavy” rain threshold. Extreme rainfall rates can reduce  $\mu_B$  so significantly that landings in such conditions are best avoided. However, to make this operational decision, flight crews need to be made aware of the presence of extreme rainfall conditions through more precise rainfall rate descriptors, and the effect of extreme rainfall on  $\mu_B$  should be reflected in the RCAM.

### Calculating the $\mu_B$ achieved during a landing ground roll

Fig. 1 is a free-body diagram showing the forces and moments acting on an airplane during the braking portion of the ground roll following a landing. Applying Newton’s second law in the body-axis system shown in Fig. 1 yields the following system of equations:

$$F_N = \mu_N N_N \quad [1]$$

$$F_M = \mu_B N_M \quad [2]$$

$$\sum F_x = W n_x + W_x = W(n_x - \sin \theta) \quad [3]$$

$$\sum F_z = W n_z + W_z = W(n_z + \cos \theta) \quad [4]$$

$$\sum M_y = 0 \quad [5]$$

Where:

$N_N$  = vertical reaction at nose gear

$\mu_N$  = rolling friction coefficient at nose gear

$F_N$  = longitudinal reaction at nose gear (rolling friction on nose gear)

$N_M$  = vertical reaction at main gear

$\mu_B$  = wheel braking friction coefficient at main gear

$F_M$  = longitudinal reaction at main gear (braking force on main gear)

- $\sum F_x$  = sum of forces along body x-axis  
 $W$  = airplane weight  
 $W_x$  = component of airplane weight along body x-axis  
 $n_x$  = longitudinal load factor  
 $\theta$  = airplane pitch angle  
 $\sum F_z$  = sum of forces along body z-axis  
 $W_z$  = component of airplane weight along body z-axis  
 $n_z$  = vertical load factor (= normal load factor multiplied by -1)  
 $\sum M_y$  = sum of moments about body y-axis

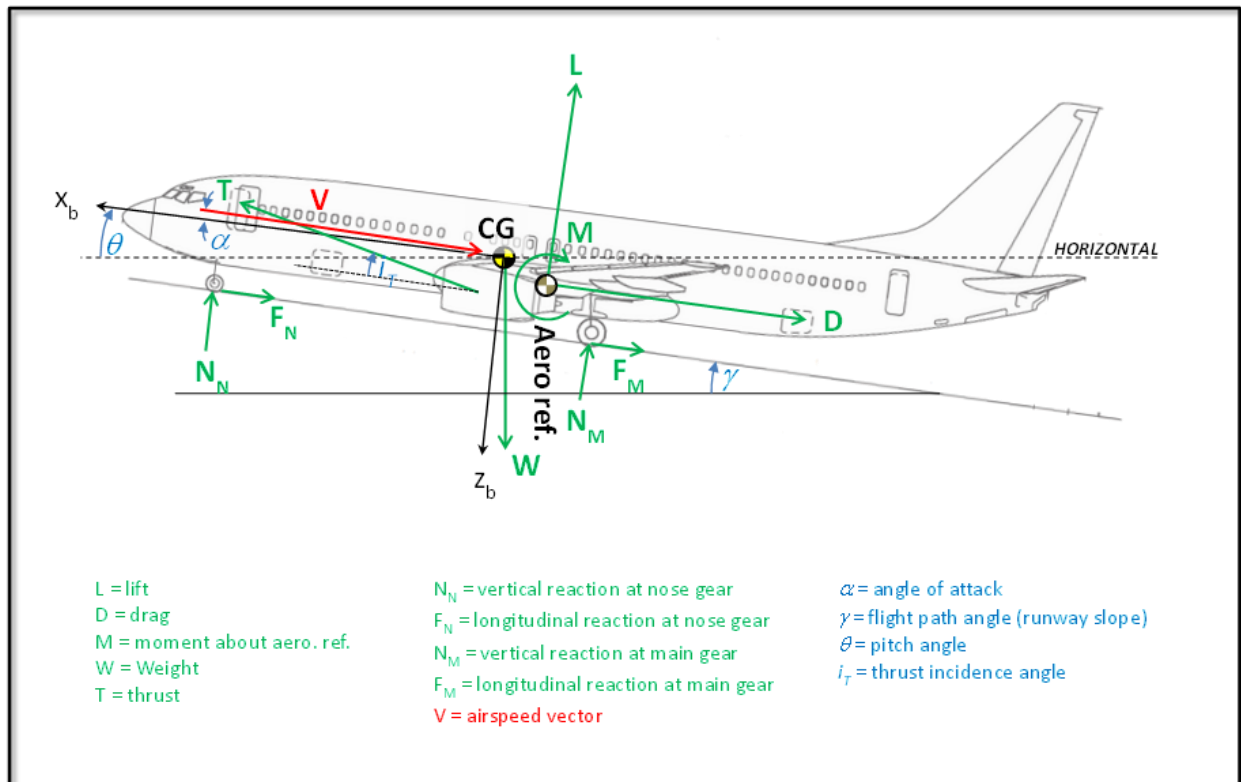


**Figure 1.** Free body diagram of forces on airplane during ground roll.

Note from Eq. (2) that the retarding force provided by the main gear tires during braking ( $F_M$ ) is equal to the normal force on the gear,  $N_M$  (acting perpendicular to the runway surface), multiplied by  $\mu_B$ .  $N_M$  is approximately equal to the weight of the airplane, minus the lift provided by the wings (see Fig. 1). The lift depends on the flap setting, angle of attack ( $\alpha$ ), dynamic pressure (airspeed and air density), and the position of the spoilers or speedbrakes (if the airplane is so equipped). Deploying the spoilers or speedbrakes after landing greatly improves braking by reducing the airplane's lift, thereby increasing  $N_M$  (and  $F_M$ ).

For the overrun events considered in this paper, the  $\mu_B$  developed during the ground roll can be computed from  $\theta$ ,  $n_x$  and engine N1 data recorded on the Flight Data Recorder (FDR), and knowledge of the airplane's aerodynamic and thrust characteristics. The vertical and longitudinal

reaction forces at the main and nose gear ( $N_N$ ,  $F_N$ ,  $N_M$ , and  $F_M$ ) are unknown, but can be computed by solving Eqs. [1]-[5]. Assuming a typical value for rolling friction on the nose gear ( $\mu_N$ ),<sup>4</sup> Equations [1]-[5] can be reduced to three equations for the three unknowns  $N_N$ ,  $N_M$ , and  $\mu_B$ . As is evident in Fig. 1, the geometry of the landing gear, thrust line, center of gravity (CG) location, and aerodynamic reference point of the airplane must be known. This geometry, as well as aerodynamic coefficient and thrust data, is generally available from the manufacturers of the airplanes involved in the events being investigated. The runway gradient, which on the ground is equivalent to the flight path angle ( $\gamma$ ), is needed along with the recorded  $\theta$  to compute  $\alpha$ , and can be obtained from airport survey data.

The results of solving Eqs. [1]-[5] for  $\mu_B$  in several overrun cases are presented below.

### Physical parameters affecting $\mu_B$ on a wet runway: ESDU models, old & new

The physical parameters affecting  $\mu_B$  have been the object of much study over the last 50 years. A convenient summary of much of this research can be found in the Engineering Science Data Unit (ESDU) Items 71025 and 71026, *Frictional and retarding forces on aircraft tires*, Parts I and II, respectively (Refs. 2 and 3).

Refs. 2 and 3 indicate that  $\mu_B$  increases above the rolling (unbraked) coefficient of friction ( $\mu_N$  in Eq.(1)) when the slip ratio ( $s$ ) of the main gear tires increases above 0, where  $s$  is given by:

$$s = 1 - \frac{V_{WHEEL}}{V_G} \quad [6]$$

Where  $V_G$  is the airplane's ground speed, and  $V_{WHEEL}$  is the tangential speed of the tire:

$$V_{WHEEL} = \omega_{WHEEL} r_{TIRE} \quad [7]$$

Where  $\omega_{WHEEL}$  is the angular velocity of the wheel, and  $r_{TIRE}$  is the effective radius of the tire (the distance from the center of rotation of the wheel to the point where the tire contacts the runway). Per Eq. [6], when the tires are free-rolling and  $V_{WHEEL} = V_G$ , then  $s = 0$ . Conversely, when the tires are locked and  $V_{WHEEL} = 0$ , then  $s = 1$ .

The  $\mu_B$  behavior described in Refs. 1, 2 and 3 can be summarized as follows:

- $\mu_B$  increases above the rolling (unbraked) coefficient of friction ( $\mu_N$  in Eq. [1]) when the slip ratio  $s$  (Eq. [6]) of the main gear tires increases above 0.
- $\mu_B$  increases to a maximum ( $\mu_{max}$ ) at a slip ratio  $s_{\mu,max}$ , and then decreases to the locked-wheel skidding coefficient of friction ( $\mu_{skid}$ ) at  $s = 1$  (see Fig. 2).
- The shape of the curve of  $\mu_B$  against  $s$  is affected by surface texture and tire tread pattern and is particularly variable in the region between  $\mu_{max}$  and  $\mu_{skid}$ .
- $\mu_{max}$  and  $\mu_{skid}$  are affected by:



- Tire design and construction (tread material, tread pattern; the tire tread pattern influences the tire's ability to move water away from the footprint of the tire).
  - Tire inflation pressure: on dry and wet runways,  $\mu_B$  tends to decrease with increasing inflation pressure; however, higher inflation pressure will increase the hydroplaning speed in standing water (see below).
  - Runway surface material and texture (roughness), including large or macro-scale texture (macrotecture), and small or micro-scale texture (microtexture) (see Fig.3).
  - Water depth on runway: on wet runways,  $\mu_B$  is a strong function of forward speed. When, in addition, the runway is flooded (water deeper than 3 mm or 0.1 inches above the top of the surface asperities), then hydroplaning is possible (see below).
  - Runway surface deposits (loose surface deposits such as sand, grit or dust decrease  $\mu_B$  on a dry surface, and may increase or decrease  $\mu_B$  on a wet surface depending on the surface texture and water depth.
  - Rubber deposits, hardened smears of asphalt binder, and paint: these deposits “can cover large areas of busy runways, particularly near the touch-down region ... in dry conditions no appreciable effects are observed. In wet conditions, large reductions may occur in both  $\mu_{max}$  and  $\mu_{skid}$ - depending in part on the initial texture of the underlying surface” [Ref. 2].
  - Forward speed: “In general,  $\mu_{max}$  and  $\mu_{skid}$  decrease with increase in forward speed” [Ref. 2], though this effect is much more pronounced on wet runways than on dry ones. The effect of speed on  $\mu_B$  on a wet runway is described further below.
  - Tire wear: “For the aircraft operator, tire wear is a most important factor ... the available  $\mu_B$  in wet conditions decreases as a tire wears. For a typical aircraft-type, rib-tread tire, when groove depths have been reduced to about 20% or less of the unworn value, the remaining tread may be ‘flattened out’ under load and the tire may then behave as if smooth” [Ref. 2].
- $s_{\mu,max}$  (see Fig. 2) usually lies between 0.1 and 0.2. Modern anti-skid braking systems are designed to detect and operate near  $s_{\mu,max}$ , but they cannot do so perfectly. The ability of these systems to operate at  $s_{\mu,max}$  is a measure of their efficiency ( $\eta_{AS}$ ).
  - The RCAM wet-runway  $\mu_B$  model assumes a constant  $\eta_{AS}$  of 80% for modern, “fully-modulating” anti-skid braking systems, over the full speed range of the airplane, and independent of the  $\mu_{max}$  that can be attained on the runway. However, the research presented in Ref. 1 suggests that  $\eta_{AS}$  can decrease as  $\mu_{max}$  decreases, and may even be as low as 0.5 at  $\mu_{max} = 0.3$ .
  - On a wet runway,  $\mu_B$  decreases precipitously with forward speed, particularly on runways with relatively low macrotecture and / or microtexture.
  - Though runway surface temperature is not addressed in Refs. 1 or ESDU 71025 or 71026, ESDU Item 05011 (Ref. 10) indicates that  $\mu_{max}$  decreases as temperature increases.

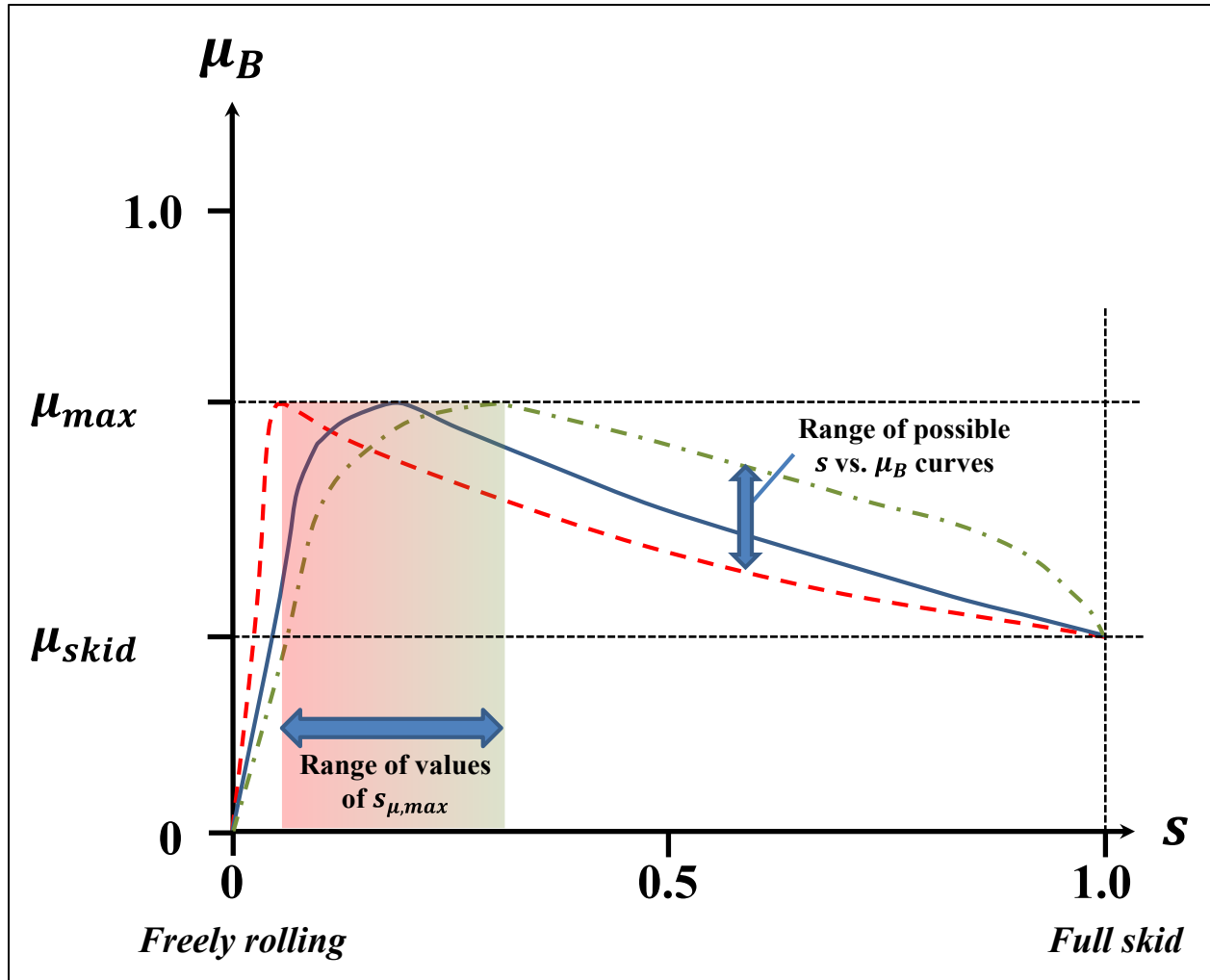


Figure 2. Effect of slip ratio  $s$  on the wheel braking friction coefficient  $\mu_B$  (adapted from ESDU 71026).

ESDU 71026 presents a semi-empirical method for determining  $\mu_{max}$ , based on curves of  $\mu_{max}$  vs. ground speed for different tire pressures and runway macrotexture (roughness) “classes.” However, the document itself notes that the scatter in this data (which might be due to, among other things, variations in the microtexture of the surfaces tested), results in a very large range of possible  $\mu_{max}$  at any given speed and tire inflation pressure.

In February 2013, ESDU issued item 10015, titled *Model for performance of a single aircraft tyre rolling or braking on dry and precipitate contaminated runways* (Ref. 9). ESDU 10015 presents a mathematical method for computing  $\mu_B$  as a function of the slip ratio  $s$ . The equations required to compute  $\mu_{max}$  on contaminated runways as a function of  $s$ , contaminant depth, microtexture and macrotexture values, runway surface temperature, and various tire parameters per the model described in ESDU 10015 are summarized in ESDU item 05011, titled *Aircraft tyre rolling or braking on dry or precipitate contaminated runways: Summary of the model* (Ref. 10). ESDU items 05011 and 10015 were amended in April 2023.

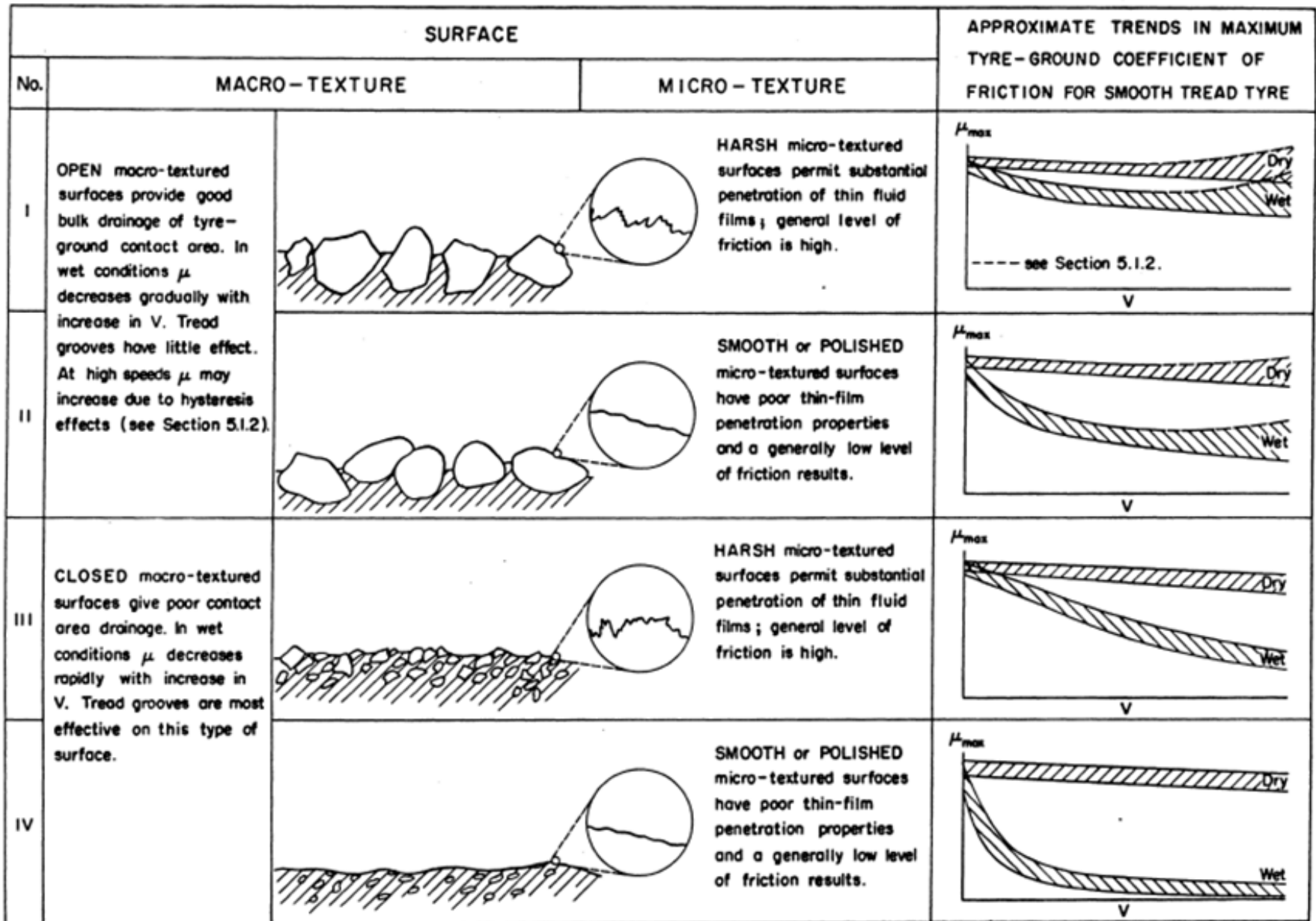


Figure 3. Effect of surface texture on  $\mu_B$ , from ESDU 71026.

In the ESDU 05011 model, the microtexture of the runway is controlled by a “microtexture sharpness parameter” (F1). The nominal value in the model is  $F1 = 0.52$ . Smaller values of F1 correspond to harsher microtextures, and larger values correspond to smoother microtextures.

As described in Ref. 4, runway macrotexture can be measured using several techniques, and the runway classes in ESDU 71026 are based on such measurements. While the significant effect of microtexture on  $\mu_{max}$  is well understood (see Figs. 3 & 7), microtexture has been difficult to quantify and measure until recently, and ESDU 71026 does not account for microtexture explicitly. Today, laser scanners are capable of measuring microtexture, though work to correlate these measurements with values of F1 in the ESDU 05011 model is ongoing (see, for example, Ref. 11). In addition, the European Aviation Safety Agency (EASA) is sponsoring research (including flight tests scheduled for Summer 2023) to develop a method for assessing runway microtexture and relating it to wet runway braking friction capabilities (see <https://www.easa.europa.eu/en/research-projects/runway-micro-texture-rwymt>).

Fig. 4 plots wet-runway  $\mu_B$  as a function of slip ratio  $s$  over a range of ground speeds, as computed using the ESDU 05011 model. Figs. 5-9 present calculations of wet-runway  $\mu_{max}$  using the ESDU 05011 model that illustrate the dependence of  $\mu_{max}$  on tire inflation pressure, runway macrotexture and microtexture, runway surface temperature, and depth of water on the runway. In each case,  $\mu_{max}$  is plotted vs.  $V_G$ , and the parameter under consideration is varied while the others are held constant. The ESDU model also requires, as inputs, the number of main gear tires, the normal force on the tires, and the tire diameter and width. Values representative of a twin-engine transport airplane weighing 145,000 pounds are used in the calculations shown here.

The pronounced decrease in wet-runway  $\mu_B$  with increasing  $V_G$  is apparent Figs. 4-9. In addition, Fig. 3 shows that (for the conditions specified) the value of  $s_{\mu,max}$  varies with  $V_G$ , from about 0.22 at  $V_G = 20$  kt. to about 0.06 at  $V_G = 160$  kt. An airplane’s anti-skid braking system is designed to vary  $s$  continuously so that the tire is always operating near  $s_{\mu,max}$ ; the anti-skid efficiency  $\eta_{AS}$  is a measure of how well this is accomplished.

ESDU 71025 explains the decrease in  $\mu_B$  with forward speed on wet runways as follows:

The presence of a fluid, which is usually water, on a runway decreases the available tire-ground coefficient of friction.

The tire-ground contact area in wet conditions can be divided into three zones, as illustrated in Fig. [10a].

*Zone 1* is the region where impact of the tire with the surface fluid generates sufficient pressure to overcome the inertia of the fluid. Much of the fluid is either ejected as spray or forced beneath the tire into the tread grooves (if present) or into the drainage paths provided by the surface texture. Throughout Zone 1 a continuous, relatively thick fluid layer exists between the tire and the runway surface and the only retarding force developed is that due to fluid drag ....

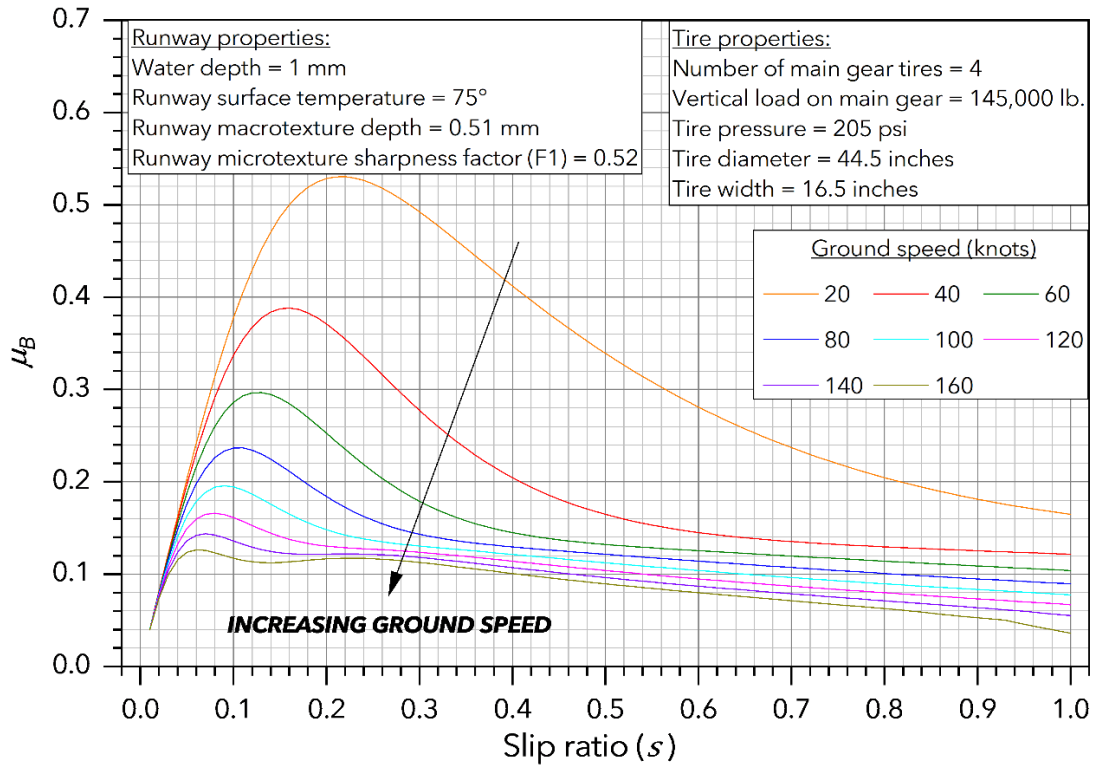


Figure 4. Variation in wet-runway  $\mu_B$  with slip ratio and ground speed, as computed using ESDU 05011.

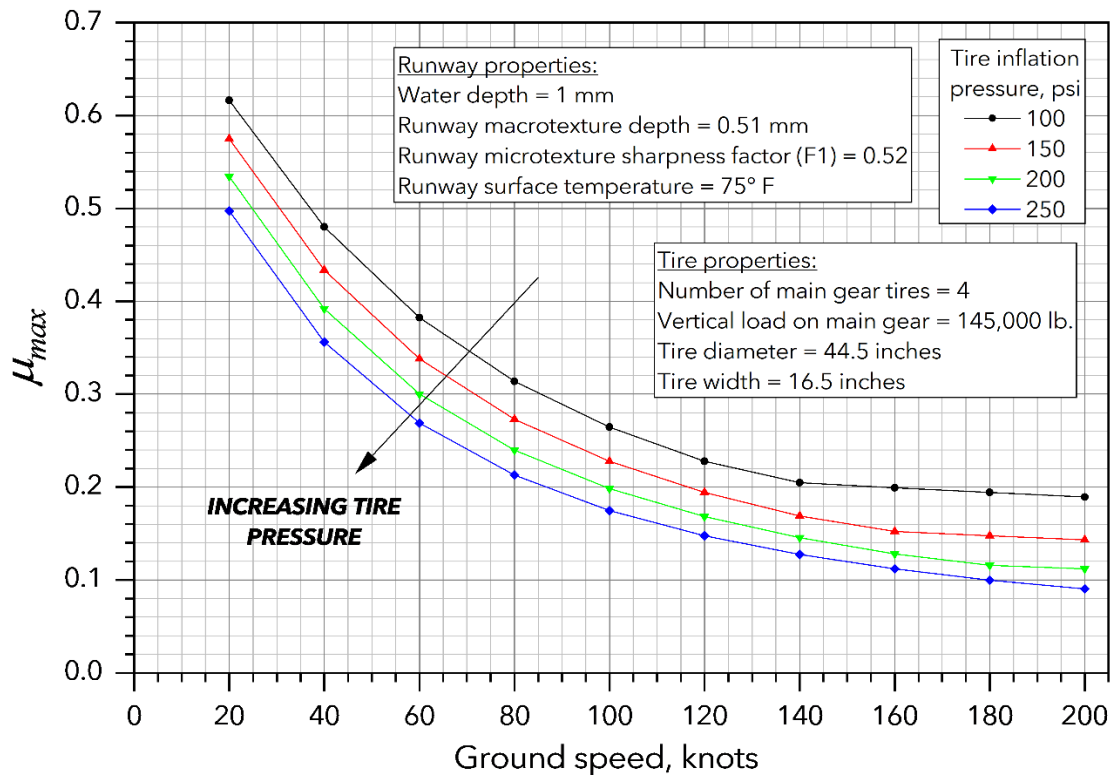


Figure 5. Variation in wet-runway  $\mu_{max}$  with tire pressure and ground speed, as computed using ESDU 05011.

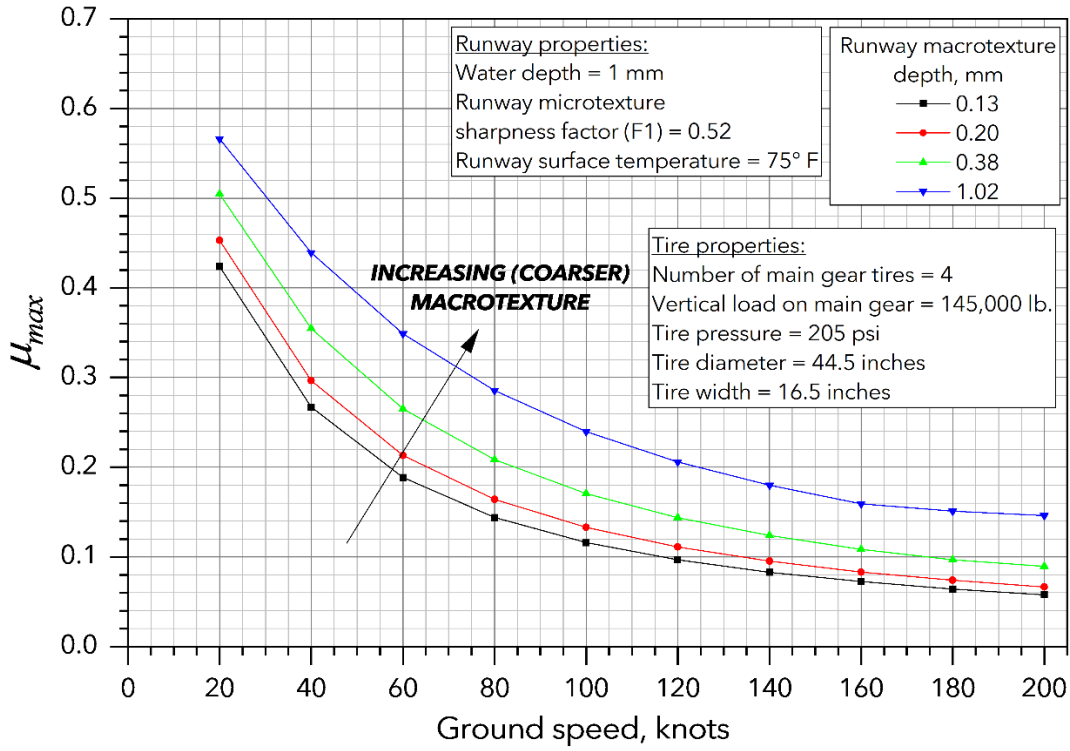


Figure 6. Variation in wet-runway  $\mu_{max}$  with runway macrotexture and ground speed, as computed using ESDU 05011.

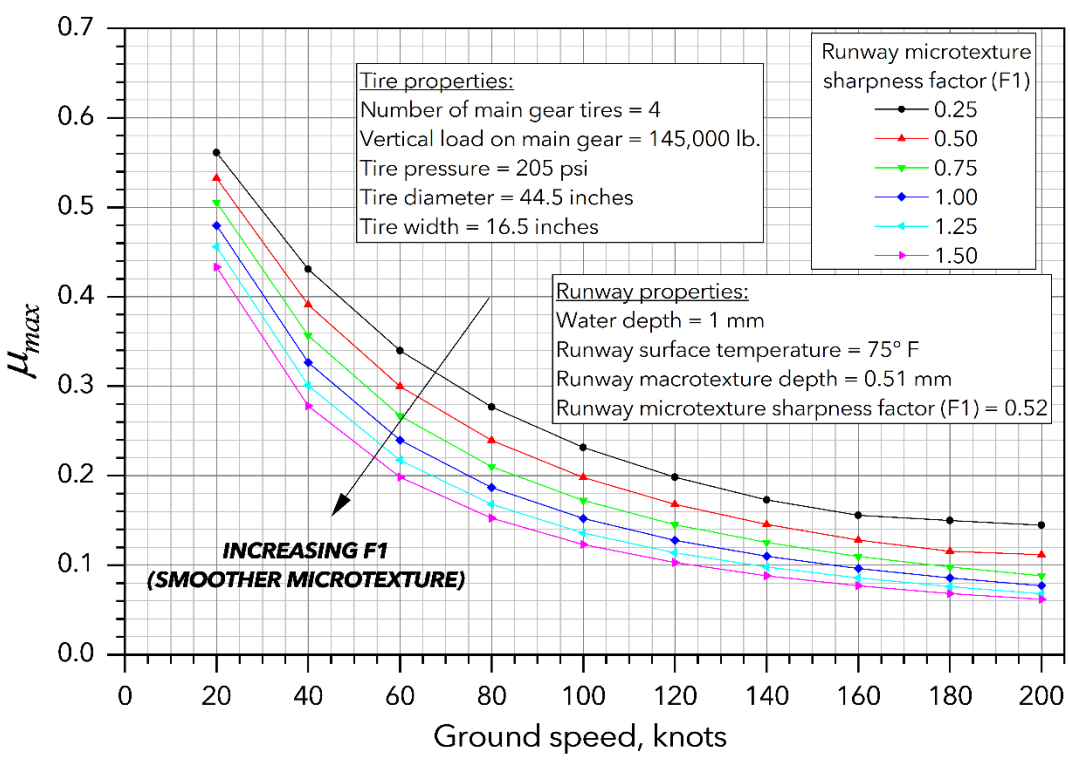
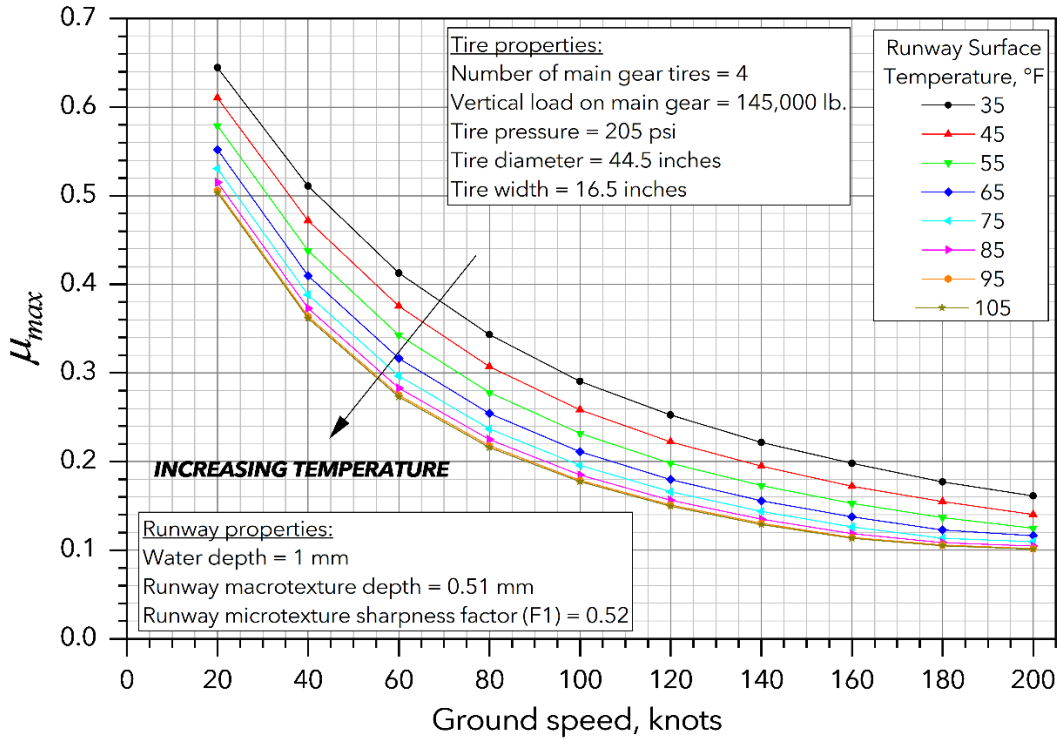
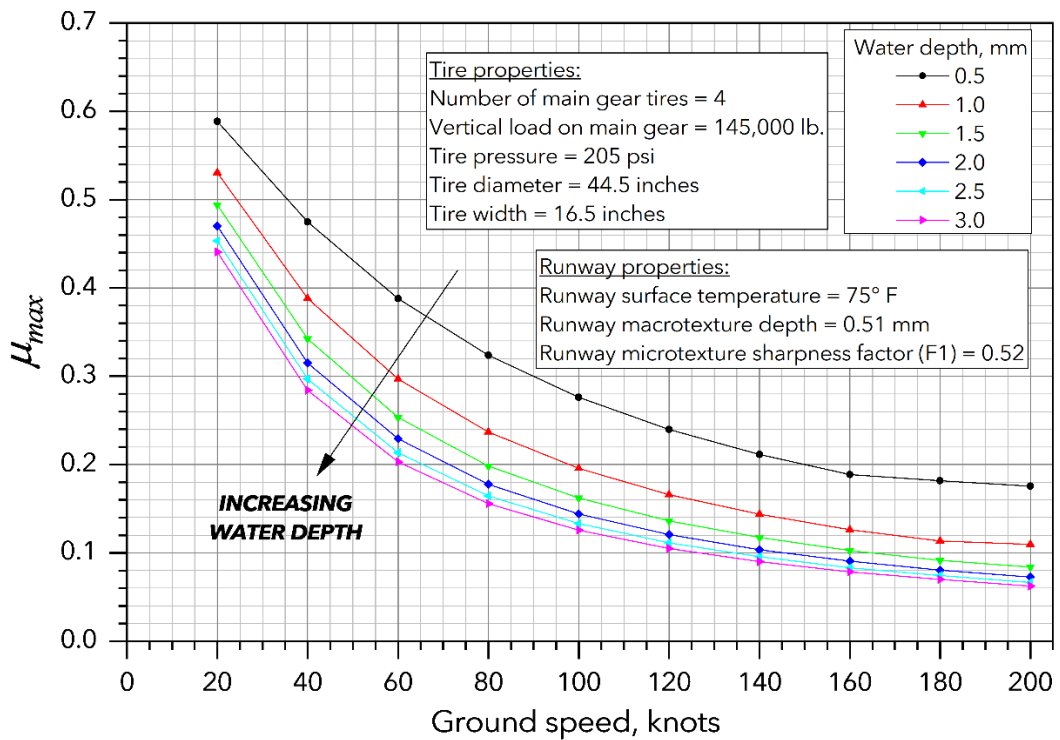


Figure 7. Variation in wet-runway  $\mu_{max}$  with runway microtexture and ground speed, as computed using ESDU 05011.



**Figure 8.** Variation in wet-runway  $\mu_{max}$  with runway surface temperature and ground speed, as computed using ESDU 05011.



**Figure 9.** Variation in wet-runway  $\mu_{max}$  with runway water depth and ground speed, as computed using ESDU 05011.

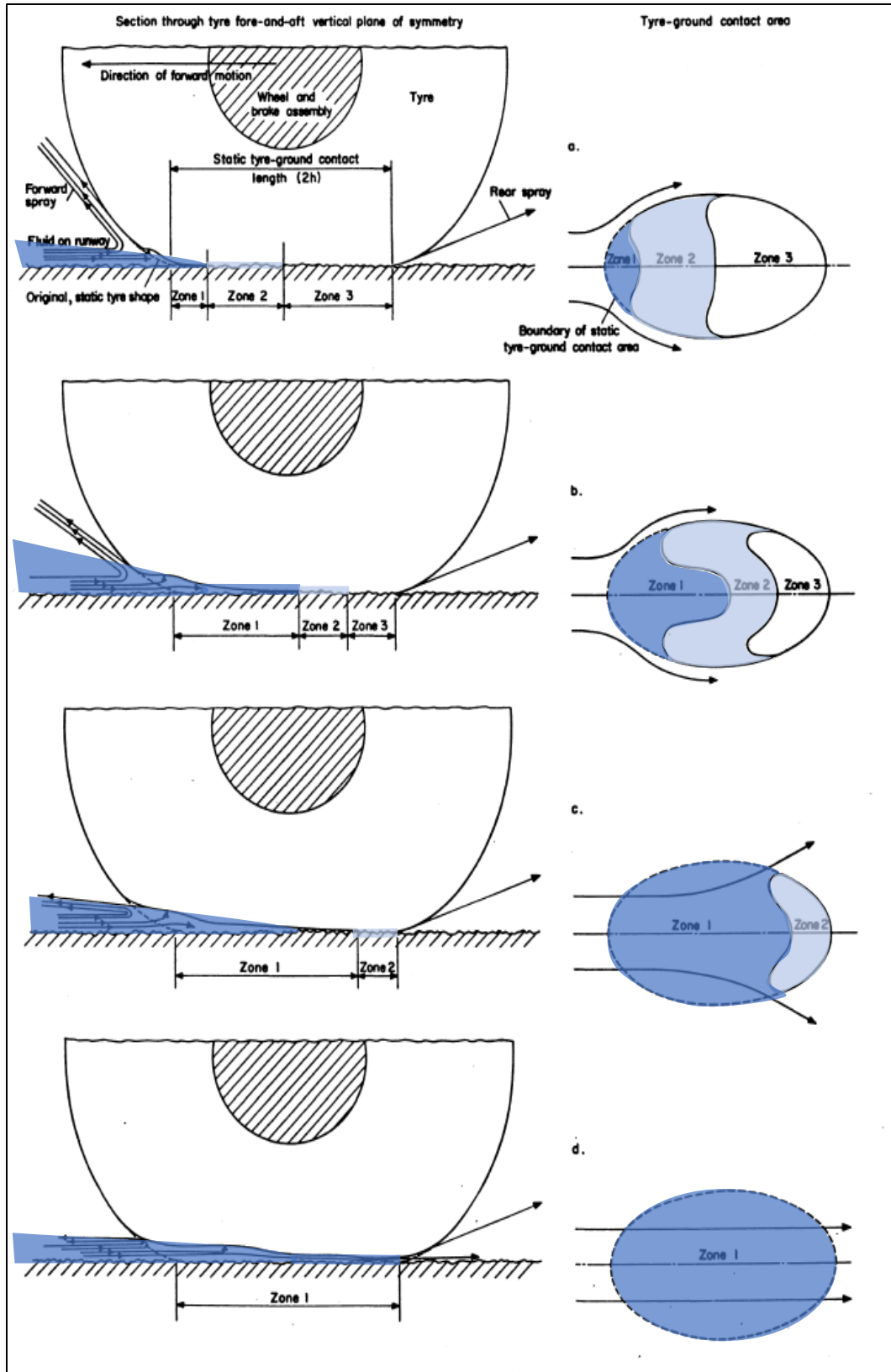


Figure 10. Effect of forward speed on the tyre-ground contact area in wet conditions, from ESDU 71025.



*Zone 2* is a transition region. After the bulk of the fluid is displaced, a thin film remains between the tire and the surface. At the rear of *Zone 1*, and in *Zone 2*, a rapid outflow of fluid is prevented, and fluid pressures are maintained, by viscous effects. The thin film first breaks down at points where the local bearing pressure is high, e.g. at sharp surface asperities. In the presence of a lubricant such as water, the coefficient of friction of rubber on hard surfaces is greatly reduced from the dry surface value and varies little with changes in sliding speed and temperature .... Thus, in general, very little frictional force is generated wherever a thin film of fluid persists.

*Zone 3* is the region of predominantly dry contact and, although obviously smaller than the contact area in dry conditions, it is here that most of the braking force is generated ....

In wet conditions, the tire-ground coefficient of friction depends on the relative sizes of *Zones 1, 2* and *3*. These are determined by the surface texture, the depth, density and viscosity of the fluid, the tread pattern and inflation pressure of the tire and the time [required] ... for a tread element to pass through the contact area ....

Figure [10] also shows the effect of increased forward speed on the relative sizes of *Zones 1, 2* and *3*. In Figure [10b] the tire forward speed is higher than in Figure [10a] so that *Zone 1* extends farther back into the contact area and *Zones 2* and *3* occupy a horseshoe-shaped region at the rear. In Figure [10c], at a still higher speed, contact with the ground is all but lost. In this condition the tire develops very little braking force. Finally, in Figure [10d], the tire is moving at a speed such that *Zone 1* extends throughout the contact area. (When dry contact with the ground ceases, the tire is said to be "planing".)

## Hydroplaning on wet runways

The discussion of hydroplaning in Ref. 1 can be summarized as follows:

- There are three types of hydroplaning: viscous hydroplaning, dynamic hydroplaning, and reverted-rubber hydroplaning.
- "Viscous hydroplaning" is associated with the buildup of water pressure under the tire due to viscosity in a thin film of water between a portion of the tire footprint and the runway surface. This is the kind of hydroplaning inferred when a surface is described as "slippery when wet," e.g., a wet bathtub.  $\mu_{max}$  is greatly reduced under the water film (as shown in Fig. 10c).
- "Dynamic hydroplaning" is associated with the buildup of water pressure due to water density and the tire's forward speed; in this condition, the tire is lifted entirely off the surface of the runway, and a continuous, relatively thick layer of water lies between the tire and the runway surface (as shown in Fig. 10d). Dynamic hydroplaning is commonly referred to simply as "hydroplaning," and can be experienced by driving a car through a deep puddle at high speed. Under dynamic hydroplaning conditions,  $\mu_{max}$  is further reduced, with the tire developing very little braking force, and the only retarding force being that due to fluid drag.
- A water depth of 3 mm above the top of the runway macrotexture is considered the minimum required to support dynamic hydroplaning. Consistent with this understanding, the RCAM model considers a runway "contaminated" with standing water (i.e., "flooded") when more than 25% of the runway surface is covered with surface water more than 3 mm (0.118 inches) deep.

- If the water depth is sufficient, dynamic hydroplaning will occur when the tire's forward speed is greater than or equal to the hydroplaning speed. In Ref. 14, W.B. Horne identifies three “zones” of hydroplaning risk based on water depth; these zones are illustrated in Fig. 22 and discussed further below.
- For rotating tires (e.g., airplanes aborting a takeoff roll), the hydroplaning speed is given by

$$V_{p,spin\ down} = 9\sqrt{p} \quad (\text{rotating tire}) \quad [8a]$$

Where  $V_p$  is in knots and  $p$  is the tire inflation pressure in psi. Ref. 18 notes that the tire tread depth can affect the hydroplaning speed, with higher tread depths corresponding to higher hydroplaning speeds.

- For nonrotating tires (e.g., airplanes on approach to landing), the hydroplaning speed is given by

$$V_{p,spin\ up} = 7.7\sqrt{p} \quad (\text{nonrotating tire}) \quad [8b]$$

- On a wet runway,  $\mu_{max}$  decreases with increasing speed due to viscous hydroplaning. If the water depth is sufficient and the speed increases to  $V_p$ , then dynamic hydroplaning will occur and  $\mu_B$  will decrease to a minimum value ( $\approx 0.05$ ; the unbraked rolling  $\mu_B$  is typically modeled as 0.0125 to 0.03).
- Tires in a dynamic hydroplaning condition may experience “spin-down,” in which unbraked wheels slow down or stop completely. This effect is due to both the absence of a spin-up moment due to friction, and the presence of a spin-down moment resulting from a shift in the center of pressure towards the front of a hydroplaning tire. This “spin-down” will cause the anti-skid system to limit the hydraulic pressure to the wheel brake to a very low level until the wheel “spins-up.”
- “Reverted-rubber” hydroplaning occurs during locked-wheel skids on wet runways when the tire rubber in the skid patches reverts to an uncured state. In this condition,  $\mu_{max}$  decreases to very low values, and the tire leaves white streaks on the runway (as opposed to black streaks on dry runways resulting from molten rubber deposited in the wheel track). The low  $\mu_{max}$  during reverted-rubber hydroplaning is relatively insensitive to airplane speed and runway texture.

### Estimating the depth of water on wet runways

As described above, if a landing airplane touches down at a ground speed greater than  $V_{p,spin\ up}$ , and if the depth of water on the runway is sufficient (about 3 mm or greater), then between touchdown and the time that the airplane decelerates through  $V_{p,spin\ up}$ , dynamic hydroplaning can occur. Further, Fig. 9 indicates that  $\mu_{max}$  decreases with water depth even in the absence of dynamic hydroplaning. Consequently, it is of interest to determine the possible depth of water on the runway when investigating an overrun event.

In steady-state conditions during a rain event, the water depth at a given point from the runway centerline is constant: the amount of water flowing towards that point from the crown (centerline) of the runway equals the amount of water flowing away from the point towards the runway edge. The volume of water per unit runway length flowing past a given point from the centerline is proportional to the speed of the water times the water depth. The water volume will increase with rainfall rate and distance from the centerline (the further from the centerline, the more runway area is available for collecting water), and the water speed will increase with the runway cross-slope. Thus, the water depth will increase with distance from the runway centerline (to accommodate the increasing volume of water) and with rainfall rate. At a given rainfall rate and distance from the centerline, the water depth will decrease as the runway cross-slope increases, since the increased speed of the water accommodates the same volume of water flow at a lesser water depth.

The runway macrotexture depth is the average depth of irregularities in the surface of the runway, produced by the coarseness of the surface texture (see Fig. 3). The greater the number and magnitude of these irregularities, the more “channels” are provided for water to flow through, and the higher the rainfall rate required to submerge the “peaks” of the irregularities. On a grooved runway, mechanically created grooves provide additional “macro-texture” to facilitate this drainage and increase the rainfall rate the runway can accept before the water depth rises above the peaks.

Under some conditions, the required water depth to accommodate the volume of water flow will be less than the average macrotexture depth of the runway; in this case, the tips of the macrotexture irregularities will be above the water. If the required water depth is greater than the macrotexture depth, then the tips of the macrotexture irregularities will be below the water.

Ref. 8 documents the results of experiments performed at the Texas Transportation Institute (TTI) that quantified the water depths resulting from various combinations of rainfall intensity, pavement cross slope, surface texture, and drainage length. The TTI report provides the following equation to describe the experimental results:

$$d = (0.00338) \left(\frac{1}{T}\right)^{-0.11} (L)^{0.43} (I)^{0.59} \left(\frac{1}{S}\right)^{0.42} - T \quad [9]$$

where:

$d$  = average water depth above the top of the macrotexture irregularities (inches);

$T$  = average macrotexture depth, inches;

$L$  = drainage path-length (i.e., distance from runway centerline), feet;

$I$  = rainfall intensity (inches / hour)

$S$  = runway cross slope, ft/ft (= slope in % divided by 100)

The results of using Eqn. [9] to evaluate the depth of water in selected overrun events considered in this paper are discussed below.

## Modeling $\mu_B$ in the TALPA and GRF frameworks

The RCAM is described in FAA Advisory Circular (AC) 25-32, *Landing Performance Data for Time-of-Arrival Landing Performance Assessments*. Before discussing how the RCAM and associated guidance material in the AC model  $\mu_B$  for different runway surface conditions, a brief review of the development of the RCAM and AC is in order.

In December 2005, Southwest Airlines (SWA) flight 1248, a Boeing 737-700, ran off the departure end of runway 31C after landing at Chicago Midway International Airport, Chicago, Illinois (KMDW). The airplane rolled through a blast fence, an airport perimeter fence, and onto an adjacent roadway, where it struck an automobile before coming to a stop. A child in the automobile was killed, one automobile occupant received serious injuries, and three other automobile occupants received minor injuries. Eighteen of the 103 airplane occupants (98 passengers, 3 flight attendants, and 2 pilots) received minor injuries, and the airplane was substantially damaged.<sup>5</sup>

The field conditions reported on the KMDW website that were most recent to the time of the accident indicated that runway 31C had a trace to 1/16 inch of wet snow over 90 percent of its surface, with 10 percent of its surface clear and wet.

Following this accident, the FAA performed an internal audit of regulations and guidance information concerning landing distance requirements, and on August 31, 2006 issued Safety Alert For Operators (SAFO) 06012, titled *Landing Performance Assessments at Time of Arrival (Turbojets)*. While a SAFO is not regulatory, it “contains important safety information and may include recommended action. SAFO content should be especially valuable to air carriers in meeting their statutory duty to provide service with the highest possible degree of safety in the public interest.” SAFO 06012

urgently recommends that operators of turbojet airplanes develop procedures for flightcrews to assess landing performance based on conditions actually existing at time of arrival, as distinct from conditions presumed at time of dispatch. Those conditions include weather, runway conditions, the airplane’s weight, and braking systems to be used. Once the actual landing distance is determined an additional safety margin of at least 15% should be added to that distance. Except under emergency conditions flightcrews should not attempt to land on runways that do not meet the assessment criteria and safety margins as specified in this SAFO.

The SAFO also notes that “the FAA has undertaken rulemaking that would explicitly require the practice described above.” As explained below, in December 2015, the FAA issued ACs 25-31 and 25-32 in lieu of the rulemaking contemplated in SAFO 06012.

SAFO 06012 points out that the dry-runway landing distances established during flight test, and that are the basis for the factored landing distances used for dispatch, are shorter than the landing distances achieved in practice. In addition, AFM landing distances for wet and contaminated runways may also be based on the minimum dry distances obtained during flight tests. Consequently, landing distances on wet or contaminated runways computed from AFM data with little or no additional safety margin may be too short for normal operations. The SAFO

recommends a conservative approach to assessing the landing distance requirements, including using the most adverse reliable braking action report or expected conditions for the runway, and using values for air distances and approach speeds that are representative of actual operations. The SAFO recommends that a 15% safety margin be then added to the computed (unfactored) landing distance, as “the FAA considers a 15% margin between the expected actual airplane landing distance and the landing distance available at the time of arrival as the minimum acceptable safety margin for normal operations.”

SAFO 06012 was cancelled and replaced by SAFO 19001, published on March 11, 2019. SAFO 19001 updates the information presented in SAFO 06012 to incorporate the RCAM framework and the corresponding contaminated runway performance guidance provided in ACs 25-31 and 25-32. As stated in SAFO 19001,

After a Boeing 737-700 runway overrun accident at Chicago Midway Airport in December 2005, the FAA convened the Takeoff and Landing Performance Assessment (TALPA) Aviation Rulemaking Committee (ARC). The Federal Aviation Administration (FAA) adopted certain recommendations of the ARC (which became known as “TALPA”), and implemented them into the National Airspace System on October 1, 2016. This SAFO provides information and guidelines to airplane operators on utilizing the safety benefits TALPA provides.

In addition,

The TALPA ARC discovered significant gaps in information needed to determine if a safe landing can be made. The ARC produced consistent terminology and runway assessment criteria, and recommended usage of non-dry, non-wet performance data for takeoff and time of arrival landing calculations. The TALPA ARC did not recommend any changes in the *preflight* landing distance requirements.<sup>6</sup>

Like SAFO 06012, SAFO 19001 recommends a conservative approach to assessing landing distance requirements, including using the most adverse reliable braking action report or runway condition code, values for air distances and approach speeds that are representative of actual operations, and a safety margin of at least 15%. However, compliance with SAFOs is not mandatory, and so the FAA can only “encourage” operators to adopt the practices recommended in the SAFO:

There is no specific regulation requiring operators to assess landing distance requirements at time of arrival, however the FAA encourages operators to adopt such procedures to ensure that a safe landing can be made. Additionally, the FAA highly encourages operators to use their FAA-approved landing performance data and any associated manufacturer-provided supplemental/advisory data in concert with the AC 91-79-generated RCAM Braking Action Codes to conduct an adequate landing distance assessment at the time of arrival. This is particularly important when the landing runway is contaminated or not the same runway analyzed for preflight calculations.

The TALPA ARC presented landing performance recommendations to the FAA in April, 2009; these recommendations are presented in detail in Ref. 4. The regulatory changes proposed by the TALPA ARC would codify many of the provisions of SAFO 06012, and introduce a new “Runway Condition and Braking Action Reports” table that would provide a mapping between a six-level

runway “code” and corresponding runway contaminant type and depth, CFME measured friction coefficient values, airplane wheel braking coefficient values, and pilot braking action reports. The runway codes range from “6,” for a dry runway, to “0,” for runways contaminated with various forms of wet ice, and for which braking action is “minimal to non-existent.” Aircraft manufacturers would have to supply data from which “operational” (i.e., unfactored) landing distances could be calculated for runway codes 6 through 1; operations would be prohibited on code “0” runways. The methods and assumptions to be used for generating this data would be specified in new regulations added to 14 CFR Part 25, “airworthiness standards: transport category airplanes.” Specifically, the new rules would require that the braking coefficients on wet runways be computed per the method described in 14 Code of Federal Regulations (CFR) §25.109 (this method is presented below).

In addition, pilots would be required to perform an en-route landing distance assessment prior to landing. This assessment would “consider the runway surface condition, aircraft landing configuration, and meteorological conditions, using approved operational landing performance data in the Airplane Flight Manual supplemented as necessary with other data acceptable to the Administrator.” A 15% safety margin would be added to the computed operational landing distance to determine the runway length required for landing.

The FAA declined to pursue rulemaking to codify the TALPA ARC recommendations, deciding instead to encourage adoption of the practices recommended by the TALPA ARC through non-regulatory means (see Ref. 4 for a detailed description of this evolution). These efforts culminated in the publication of AC 25-32, *Landing Performance Data for Time-of-Arrival Landing Performance Assessments*, in December 2015.<sup>7</sup> This AC provides guidance and standardized methods that data providers, such as type certificate (TC) holders, supplemental type certificate (STC) holders, applicants, and airplane operators can use when developing contaminated runway landing performance data for transport category airplanes. In addition, the AC includes a Runway Condition Assessment Matrix (RCAM) that is the outgrowth of the “Runway Condition and Braking Action Reports” table proposed by the TALPA ARC. The RCAM promotes the use of consistent terminology for runway surface conditions used among data providers and FAA personnel, and is presented here as Fig. 11. The FAA officially started reporting runway conditions for Part 139 airports using the RCAM in October 2016.

Note that while AC 25-32 provides guidance for the development of airplane landing performance data on contaminated runways, it does not include any operational guidance as to how this data should be used for en-route landing distance assessments, or recommend that any specific safety factor be applied to the data (whereas the TALPA ARC specifically recommended *requiring* that a safety margin of 15% be added to landing distance assessments). Similarly, the 15% safety margin and en-route landing distance assessment practice is *recommended* by SAFO 19001, but is not *required*. The NTSB expressed concern regarding these points, and about the non-regulatory approach to the TALPA ARC recommendations in general, in comments submitted to the FAA during the AC 25-32 draft comment period (see Ref. 5).

Runway Condition Code	Runway Surface Condition Description	Pilot-Reported Braking Action	Wheel Braking Coefficient
6	Dry	—	90% of certified value used to comply with § 25.125 <sup>1</sup> .
5	Frost Wet (includes damp and 1/8" (3 mm) depth or less of water) 1/8" (3 mm) depth or less of: Slush Dry snow Wet snow	Good	Per method defined in § 25.109(c).
4	-15 °C and colder outside air temperature: Compacted snow	Good to Medium <sup>2</sup>	0.20 <sup>3</sup>
3	Wet ("Slippery When Wet" runway) Dry snow or wet snow (any depth) over compacted snow Greater than 1/8" (3 mm) depth of: Dry snow Wet snow Warmer than -15 °C outside air temperature: Compacted snow	Medium <sup>2</sup>	0.16 <sup>3</sup>
2	Greater than 1/8" (3 mm) depth of: Water Slush	Medium <sup>2</sup> to Poor	For speeds below 85% of the hydroplaning speed <sup>4</sup> : 50% of the wheel braking coefficient determined in accordance with § 25.109(c), but no greater than 0.16 <sup>3</sup> ; and For speeds at 85% of the hydroplaning speed <sup>4</sup> and above: 0.05 <sup>3</sup> .
1	Ice	Poor	0.08 <sup>3</sup>
0	Wet ice Water on top of compacted snow Dry snow or wet snow over ice	Nil	Not applicable. (No operations in Nil conditions.)

<sup>1</sup> 100% of the wheel braking coefficient used to comply with § 25.125 may be used if the testing from which that braking coefficient was derived was conducted on portions of runways containing operationally representative amounts of rubber contamination and paint stripes.

<sup>2</sup> The braking action term "FAIR" is in the process of being changed to "MEDIUM" throughout the FAA. Until an official change is published, the term "FAIR" should be used.

<sup>3</sup> These wheel braking coefficients assume a fully modulating anti-skid system. For quasi-modulating systems, multiply the listed braking coefficient by 0.625. For on-off systems, multiply the listed braking coefficient by 0.375. (See AC 25-7C to determine the classification of an anti-skid system.) Airplanes without anti-skid systems will need to be addressed separately on a case-by-case basis.

<sup>4</sup> The hydroplaning speed,  $V_p$ , may be estimated by the equation  $V_p = 9\sqrt{P}$ , where  $V_p$  is the ground speed in knots and  $P$  is the tire pressure in lb/in<sup>2</sup>.

**Figure 11.** Runway Surface Condition–Pilot Reported Braking Action—Wheel Braking Coefficient Correlation Matrix, from AC 25-32.

Several of the runway condition codes (RwyCCs) and corresponding  $\mu_B$  models listed in Fig. 11 are relevant to wet-runway overrun accidents, and are discussed below.

**RwyCC 5:** This RwyCC is associated with a pilot-reported braking action of “good,” and includes a runway surface that is “wet (includes damp  $\frac{1}{8}$ ” (3 mm) depth or less of water).” For a RwyCC 5 runway, Fig. 11 indicates that the  $\mu_B$  should be computed “per [the] method defined in §25.109(c).” This method is presented below. As discussed in detail in Refs. 1 and 4, and acknowledged in SAFOs 15009 and 19003 (discussed below), the §25.109(c)  $\mu_B$  model can significantly overestimate the  $\mu_B$  available on some wet runways. In comments on the draft versions of ACs 25-31 and 25-32, the NTSB expressed concern with the use of the §25.109(c)  $\mu_B$  model for code 5 runways, given the evidence from multiple events that this model is insufficiently conservative (see Ref. 5).

**RwyCC 3:** This RwyCC is associated with a pilot-reported braking action of “medium,” and includes a “Slippery When Wet” (SWW) runway. The  $\mu_B$  for this condition is modeled as a constant 0.16. A SWW runway is defined in Advisory Circular 150/5200-30D, *Airport Field Condition Assessments and Winter Operations Safety*, and is so designated when portions of the runway fall below a minimum friction level measured with CFME.

**RwyCC 2:** This RwyCC is associated with a pilot-reported braking action of “medium to poor,” and includes a flooded runway (i.e., greater than  $\frac{1}{8}$  inch (3 mm) of water), on which dynamic hydroplaning is possible. At speeds at and above 85% of the hydroplaning speed,<sup>8</sup>  $\mu_B$  is constant at 0.05; and below 85% of the hydroplaning speed,  $\mu_B$  is modeled as “50% of the wheel braking coefficient determined in accordance with §25.109(c), but no greater than 0.16.”

**RwyCC 1:** This RwyCC is associated with a pilot-reported braking action of “poor,” and is associated with an ice-covered runway.  $\mu_B$  is modeled as a constant 0.08.

**RwyCC 0:** This RwyCC is associated with a pilot-reported braking action of “nil,” and is associated with wet ice, water on top of compacted snow, and dry or wet snow over ice. The  $\mu_B$  for this RwyCC is not modeled because it is “not applicable. (No operations in Nil conditions.)”

The ICAO Global Reporting Format (GRF) has its roots in the work of the ICAO Friction Task Force starting in 2008, and is centered around the same RCAM published in AC 25-32. The worldwide applicability date for the GRF was November 4, 2021. For more information about the development and implementation of the GRF, see <https://www.icao.int/safety/Pages/GRF.aspx>.

### **Wet-runway $\mu_B$ defined in 14 CFR 25.109**

Per Fig. 11, an RCAM RwyCC of 5 includes a runway surface that is “wet (includes damp  $\frac{1}{8}$ ” (3 mm) depth or less of water),” and for which  $\mu_B$  should be computed “per [the] method defined in §25.109(c).”



14 CFR §25.109 defines the accelerate-stop distance for transport-category airplanes, and describes how this distance is to be determined. The accelerate-stop distance is the distance required to accelerate from a stop to  $V_1$ ,<sup>9</sup> and then bring the airplane back to a stop in the remaining runway length.<sup>10</sup> §25.109(a) defines the accelerate-stop distance on a dry runway, and §25.109(b) defines the accelerate-stop distance on a wet runway. §25.109(c) defines the  $\mu_B$  to be assumed in the calculation of the accelerate-stop distance for a smooth, wet runway (the  $\mu_B$  for wet runways that are grooved or treated with porous friction course material is defined in §25.109(d)).

The §25.109(c)  $\mu_B$  model is based on the methods of ESDU 71026 (Ref. 3) (a history of this development is given in Ref. 6). For a smooth, wet runway, §25.109(c) defines the  $\mu_B$  as follows:

$$\mu_B = (\mu_{max})(\eta_{AS}) \quad [10]$$

Where  $\mu_{max}$  is the maximum  $\mu_B$  that can be achieved on the runway, and  $\eta_{AS}$  is the anti-skid system efficiency.  $\mu_{max}$  is defined in terms of cubic polynomial functions of the ground speed ( $V_G$ ), where the polynomial coefficients depend on the tire inflation pressure; higher inflation pressure results in lower  $\mu_{max}$  at a given  $V_G$ .

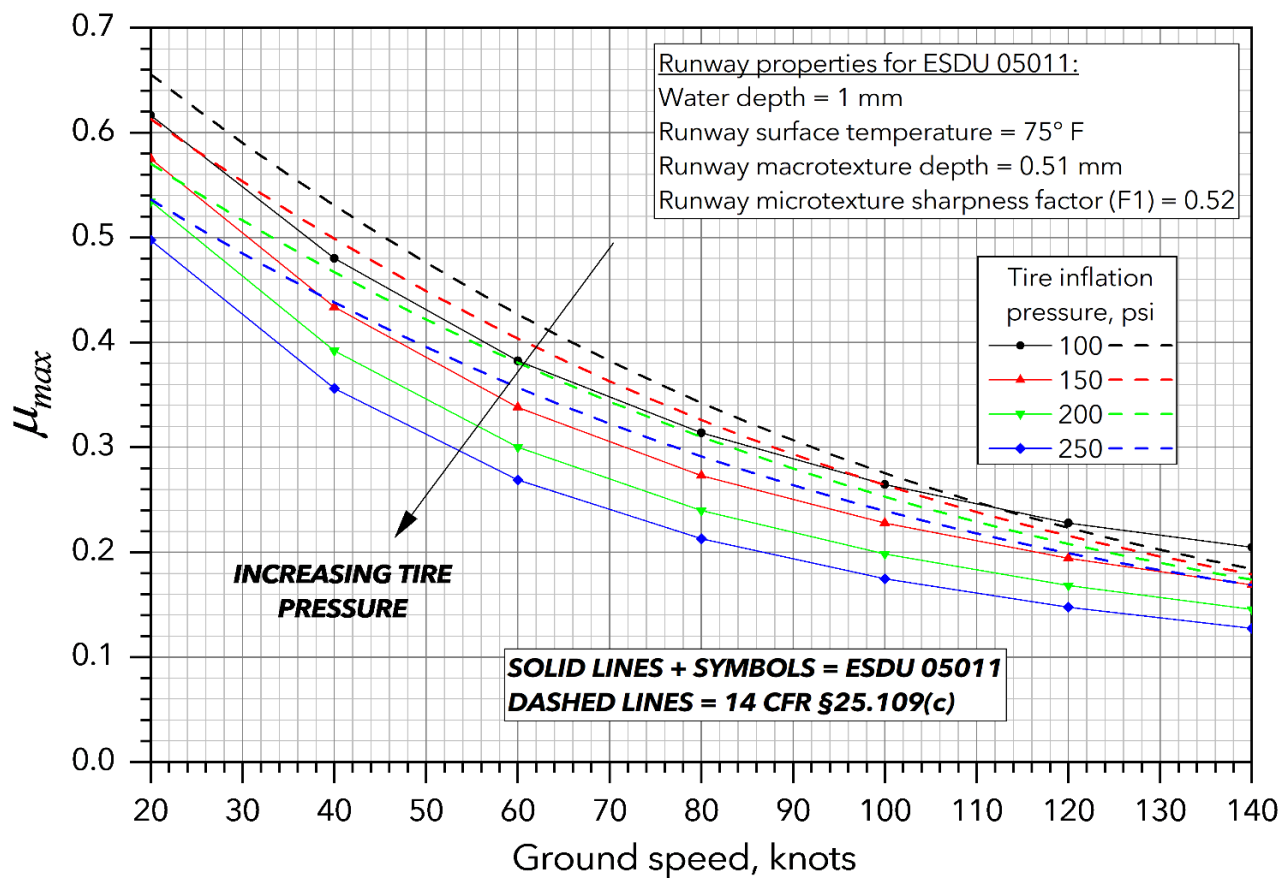


Figure 12. Comparison of wet-runway  $\mu_{max}$  based on §25.109(c) and on ESDU 05011.

The §25.109(c)  $\mu_{max}$  for tire inflation pressures of 100, 150, 200, and 250 psi are depicted by the dashed lines in Fig. 12, and compared to the  $\mu_{max}$  computed using ESDU 05011 for the same tire pressures (and for the other conditions listed in the Figure). As noted above, many variables can affect the  $\mu_{max}$  computed using ESDU 05011, so it is not surprising that the §25.109(c)  $\mu_{max}$  and the ESDU 05011  $\mu_{max}$  differ in this Figure.

Per §25.109(c), the anti-skid system efficiency  $\eta_{AS}$  in Eq. [10] can be determined by flight test, or can be assumed based on the type of anti-skid system installed (“On-Off,” “Quasi-Modulating,” or “Fully Modulating”). Modern anti-skid systems are all “Fully Modulating,” corresponding to an  $\eta_{AS}$  of 80%. FAA AC 25-7D, *Flight Test Guide for Certification of Transport Category Airplanes*, describes the three types of anti-skid braking systems identified in §25.109.<sup>11</sup>

### NASA $\mu_B$ model based on Continuous Friction Measurement Equipment (CFME) data

Ref. 1 documents six wet runway overrun events as well as the results of two wet runway braking test programs (all involving turbojet airplanes), and notes that in each case the  $\mu_B$  achieved was less than the  $\mu_B$  underlying the wet runway landing distances published in the AFMs, and the  $\mu_B$  specified by 14 CFR §25.109. Ref. 1 concludes that the reduced  $\mu_B$  can be explained by (1) a wet-runway  $\eta_{AS}$  that is significantly less than 80%; (2) a wet-runway  $\mu_{max}$  that is significantly less than what would be expected based on the pavement macrotexture and airplane tire inflation pressure in each case; or (3) a combination of these factors.

Ref. 1 also notes that the achieved  $\mu_B$  levels *are* generally consistent with the  $\mu_B$  predicted using a National Aeronautics and Space Administration (NASA)  $\mu_B$  model that is based on runway friction measurements taken with CFME. These findings are presented here in Figs. 14-19. Since the publication of Ref. 1, the NASA model has also accurately predicted the  $\mu_B$  achieved by a Boeing 737 that overran a wet, grooved runway in Burbank, California, in 2018, but has failed to predict the  $\mu_B$  achieved by a Boeing 737 that overran a wet, smooth runway (with very heavy rainfall) in Jacksonville, Florida in 2019 (see Figs. 20 & 21). The Ref. 1 events and these additional cases are considered in more detail below.



(a) Neubert Aero Corporation Dynamic Friction Tester



(b) Sarsys Surface Friction Tester

**Figure 13.** (a) Towed and (b) self-contained CFME devices.

CFME evaluate the friction level of a runway by measuring the drag forces on a braked or yawed tire that is towed or driven down the runway, while wetting the runway just ahead of the tire to a target water depth. Different types of CFME have been designed; some consist of a trailer towed behind an airport vehicle, and others have the test tire built into the vehicle itself (see Fig. 13).

The NASA method for estimating the  $\mu_B$  of an airplane from CFME measurements is described in Ref. 7, and consists of computing the ratio of the wet-runway  $\mu$  ( $\mu_{wet}$ ) to the dry-runway  $\mu$  ( $\mu_{dry}$ ) using the CFME-measured  $\mu_{wet}$  and a “characteristic  $\mu_{dry}$ ” for the CFME, and then assuming that this ratio also applies to the  $\mu_{wet}/\mu_{dry}$  ratio of the braked airplane tires. The  $\mu_{dry}$  of the airplane tires is a function of the tire inflation pressure. The “characteristic  $\mu_{dry}$ ” for different types of CFME is determined by very slow-speed  $\mu$  measurements on a dry surface.

The airplane ground speed associated with each  $\mu_{wet}$  value is similarly based on computing the ratio of the ground speed ( $V_G$ ) to the spin-down hydroplaning speed ( $V_{p,spin\ down}$ ) of the CFME, and then applying that same ratio to the spin-down hydroplaning speed of the aircraft tires. The  $V_{p,spin\ down}$  of both the CFME and airplane tires are a function of each vehicle’s tire inflation pressure (see Eq. [8a]).

In sum, the NASA  $\mu_B$  model is based on the assumption that the  $\mu_{wet}/\mu_{dry}$  and  $V_G/V_{p,spin\ down}$  ratios of CFME and airplanes are similar. The resulting airplane  $\mu_{wet}$  is the maximum wet friction coefficient that the runway can provide (equivalent to  $\mu_{max}$  in the §25.109(c) model), as a function of the airplane’s  $V_G$ :

$$\left. \frac{\mu_{max}}{\mu_{dry}} \right|_{airplane} = \left. \frac{\mu_{wet}}{\mu_{dry}} \right|_{CFME} \quad [11]$$

$$\left. \frac{V_G}{V_{p,spin\ down}} \right|_{airplane} = \left. \frac{V_G}{V_{p,spin\ down}} \right|_{CFME} \quad [12]$$

As described in §25.109(c), the actual  $\mu_B$  achieved by an aircraft is less than  $\mu_{max}$  because the braking systems of aircraft are not 100% efficient. In the NASA model,  $\mu_B$  is computed from  $\mu_{max}$  using the following equations:

$$\text{For } \mu_{max} < 0.7: \quad \mu_B = 0.2\mu_{max} + 0.7143(\mu_{max})^2 \quad [13a]$$

$$\text{For } \mu_{max} \geq 0.7: \quad \mu_B = 0.7\mu_{max} \quad [13b]$$

This computation of  $\mu_B$  from  $\mu_{max}$  to account for the braking system efficiency of the airplane is similar to the method prescribed in §25.109(c) for the computation of  $\mu_B$  by multiplying  $\mu_{max}$  by  $\eta_{AS}$  (see Eq. [10]). The  $\eta_{AS}$  implied in Eqns. [13a] and [13b] can be gleaned by dividing these equations by  $\mu_{max}$ :

$$\text{For } \mu_{max} < 0.7: \quad \eta_{AS} = \mu_B / \mu_{max} = 0.2 + 0.7143\mu_{max} \quad [14a]$$

$$\text{For } \mu_{max} \geq 0.7: \quad \eta_{AS} = \mu_B / \mu_{max} = 0.7 \quad [14b]$$

Note that the  $\eta_{AS}$  defined by these equations is a function of  $\mu_{max}$  (and is never greater than 0.7), and does not depend on the type of anti-skid braking system, as does the anti-skid efficiency value defined in §25.109(c). Significantly, Equation [14a] indicates that  $\eta_{AS}$  deteriorates with  $\mu_{max}$ ; so, as the runway gets more slippery, the anti-skid system becomes less able to take advantage of the available friction that remains – in effect, a double penalty. Ref. 4 presents additional evidence that  $\eta_{AS}$  deteriorates with  $\mu_{max}$ , contrary to the constant  $\eta_{AS}$  assumed in the §25.109(c)  $\mu_B$  model.

### Combined NASA and §25.109(c) $\mu_B$ model

FAA AC 150/5320-12C, *Measurement, Construction, and Maintenance of Skid-Resistant Airport Pavement Surfaces*, notes that the  $\mu_{max}$  on a given runway will deteriorate over time, and recommends that airports that support turbojet traffic monitor the  $\mu_{max}$  on the runways through the use of CFME. The AC defines CFME  $\mu$  values corresponding to runway friction levels that warrant specific maintenance actions. These CFME  $\mu$  values are specified for tests conducted at vehicle speeds of 40 mph and 60 mph. Per the AC, “the lower speed determines the overall macrotexture/contaminant/drainage condition of the pavement surface. The higher speed provides an indication of the condition of the surface's microtexture. A complete survey should include tests at both speeds.”

A disadvantage of the NASA  $\mu_B$  model is that the measurement speeds of the CFME device typically transform to a relatively narrow range of airplane ground speeds. Investigators might be able to conduct additional CFME tests on a runway of interest at speeds lower than 40 mph, but typically the maximum speed that can be tested is the 60 mph specified in the AC. For a typical CFME test tire inflated to 30 psi and an aircraft tire inflated to 205 psi, the 60 mph CFME test speed will transform to an airplane  $V_G$  of 136 knots. In some cases, the  $V_G$  of the airplane on the runway can be much higher (for example, the touchdown  $V_G$  of the Boeing 737 in Jacksonville was 180 knots).

Ref. 1 presents a method for estimating the airplane  $\mu_B$  across the entire speed range of interest based on a combination of the §25.109(c) model and CFME runs that address only part of the desired speed range. In this method, CFME  $\mu$  measurements are used to predict the airplane  $\mu_B$  at the airplane  $V_G$  corresponding to the CFME speed of the measurements, per the NASA CFME method described above. The  $\mu_{max}$  predicted by the §25.109(c) model at the same  $V_G$  is also computed. The CFME prediction, which is based on measurements of the particular runway of interest, can be used to compute an “effective”  $\eta_{AS}$  that should be applied to the §25.109(c)  $\mu_{max}$ , which models runways in general. This effective  $\eta_{AS}$ , termed  $k_B$ , is defined as

$$k_B = \frac{\mu_{B,CFME}}{\mu_{max,25.109}} \quad [15]$$

Where:

$\mu_{B,CFME} = \mu_B$  obtained from the CFME runs using the NASA CFME method

$\mu_{max,25.109} = \mu_{max}$  from the §25.109(c) model

If CFME measurements are only available at a single speed, then only one  $k_B$  value can be computed, and this value is used as  $\eta_{AS}$  in Eqn. [10] to compute the airplane  $\mu_B$  at any  $V_G$ . If CFME runs at both 40 and 60 mph are available, the  $k_B$  computed from each might be slightly different, in which case they could be averaged to obtain the  $\eta_{AS}$  to be used in Eqn. [10]. Alternatively, the  $k_B$  corresponding to the 40 mph run could be used for its equivalent airplane  $V_G$  and lower speeds, the  $k_B$  corresponding to the 60 mph run could be used for its equivalent airplane  $V_G$  and higher speeds, and linear interpolation could be used to compute  $k_B$  in between these speeds. If CFME runs at additional speeds are obtained, these could be used to define a curve-fit of  $k_B$  vs.  $V_G$ .

In addition, since CFME  $\mu$  measurements vary along the runway (both because of “noise” in the measurements and because some sections of the runway can in fact be more or less slippery than others), it is also possible to compute  $k_B$  as a function of location on the runway, as will be described further below.

### Comparisons of actual and modeled $\mu_B$

Figs. 14-21 present comparisons of actual and modeled  $\mu_B$  for the eight wet-runway overrun events listed in Table 2:

Date (m/d/y)	Location (runway)	Aircraft	Rainfall rate (in./hr.)	Rainfall descriptor	Runway surface	NTSB / foreign agency reference
07/31/2008	Owatonna, MN (KOWA 30)	BAe 125-800A	0.27	Moderate	Smooth	DCA08MA085
12/22/2009	Kingston, Jamaica (MKJP 12)	B737-800	0.49	Heavy	Smooth	DCA10RA017 / JCAA JA-2009-09
06/16/2010	Ottawa, Ontario (CYOW 07)	EMB-145	0.31	Heavy	Smooth	DCA10RA069 / TSB A10H004
04/26/2011	Chicago, IL (KMDW 13C)	B737-700	0.60	Heavy	Grooved	DCA11IA047
09/19/2014	Conroe, TX (KCXO 1)	EMB-505	0.24 - 0.30	Moderate to heavy	Smooth	CEN14FA505
11/21/2014	Sugar Land, TX (KSGR 35)	EMB-500	0.12	Light	Smooth	CEN15LA057
12/06/2018	Burbank, CA (KBUR 8)	B737-700	1.00	Heavy	Grooved	DCA19IA036
05/03/2019	Jacksonville, FL (KNIP 10)	B737-800	0.60 - 2.40	Heavy	Smooth	DCA19MA143

**Table 2.** Wet-runway overrun events considered in this paper.

The first six events listed in Table 2 are those considered in Ref. 1. The last two events occurred after the publication of Ref. 1. For more information about all eight events, search for the accident number of interest in the CAROL search tool on the NTSB website at [www.nts.gov](http://www.nts.gov).

The actual  $\mu_B$  for these accidents is computed from FDR data per Eqns. [1]-[5], and plotted in Figs. 14-21 as the black line labeled “actual  $\mu_B$  computed from FDR.” The Owatonna airplane did not have an FDR; the “actual”  $\mu_B$  for this case is approximated by selecting an  $\eta_{AS}$  in Eqn. [10] that results in a good match of other available evidence. This alternative evidence included radar data, CVR data, Enhanced Ground Proximity Warning System (EGPWS) and Flight Management System (FMS) data, weather data, ground scars, and witness statements (see Ref. 6 for details).

In Figs. 14-21, the modeled  $\mu_B$  in each case is computed using both the §25.109(c) model by itself and the “combined” NASA / §25.109(c) model. In Figs. 14-19, the  $\mu_B$  levels computed from the average CFME  $\mu$  over the length of the CFME test run are plotted at the corresponding airplane  $V_G$  as singular points. However, in Figs. 20 and 21 (the Burbank and Jacksonville cases) *all* the CFME  $\mu$  measurements collected on a test run (not just their average) are used, resulting in a computation of  $\mu_B$  as a function of the position on the runway. Hence, these results are plotted as lines instead of singular points. At runway coordinates where CFME measurements were not taken,  $\mu_B$  is computed using the  $k_B$  in Eqn. [15] corresponding to the nearest point where CFME data are available. Such coordinates are apparent in Figs. 20 and 21 where the CFME  $\mu_B$  curves become smooth (that is, where  $k_B$  becomes constant and no longer contains the “noise” inherent in the CFME measurements).

The results for all eight cases (except Burbank, Fig. 20) show that the achieved  $\mu_B$  is less than the §25.109(c)  $\mu_B$  (sometimes significantly so). This is of concern, since in the RCAM framework the runways involved would have been classified as RwyCC 5 (wet runway) based on the weather conditions at the times of the events, and the “expected”  $\mu_B$  would have been given by §25.109(c). In the Burbank case, the achieved  $\mu_B$  is between the §25.109(c)  $\mu_B$  for a smooth runway and the §25.109(d)  $\mu_B$  for a grooved runway (KBUR runway 8 is grooved).<sup>12</sup>

The results also indicate that, in every case (except Kingston, Fig. 15), the NASA CFME  $\mu_B$  approximates the actual  $\mu_B$  better than the §25.109(c)  $\mu_B$ . The Kingston CFME results are strange: except for the first third of the runway, the CFME measurements do not show the reduction in  $\mu$  with increased speed that would be expected based on the physics of wet-runway braking. Furthermore, the airplane  $\mu_B$  resulting from these measurements is quite high, above even the (often optimistic) §25.109(c)  $\mu_B$ . These puzzling results, and the fact that the NASA CFME model does match the actual  $\mu_B$  well in many other cases, suggest that the Kingston case is an anomaly.

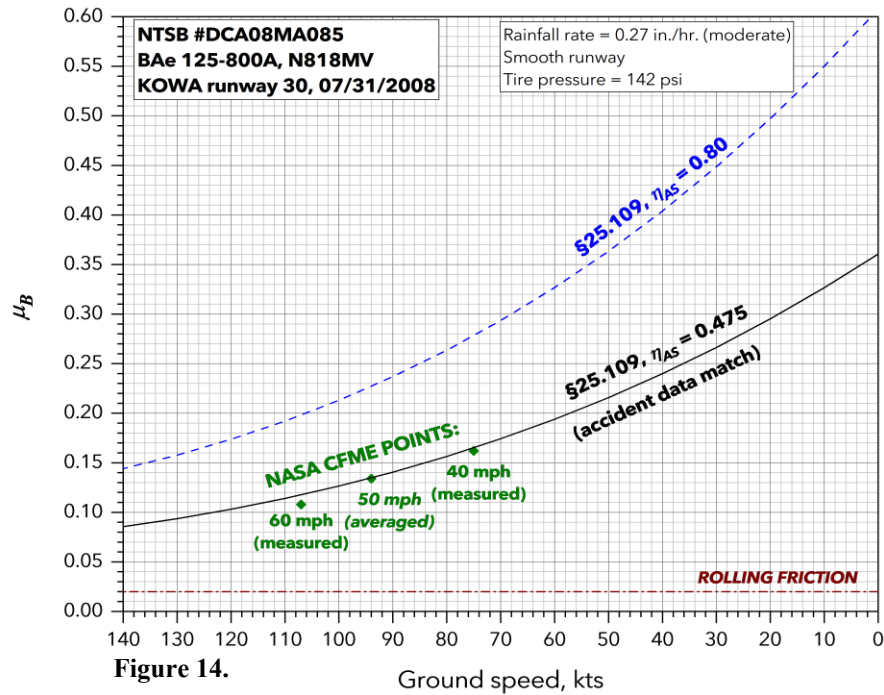


Figure 14.

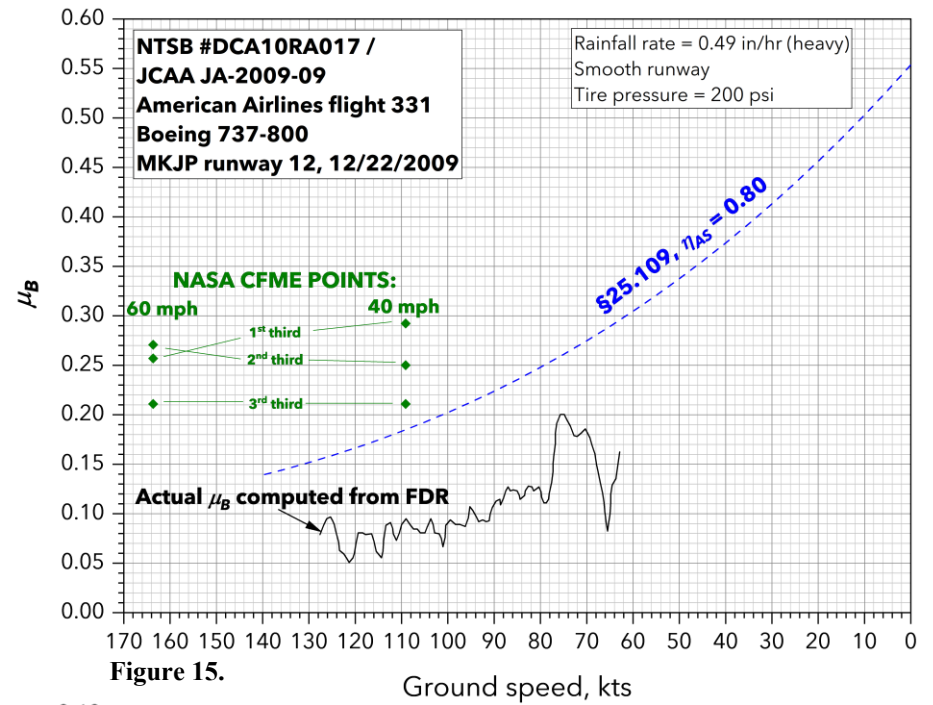


Figure 15.

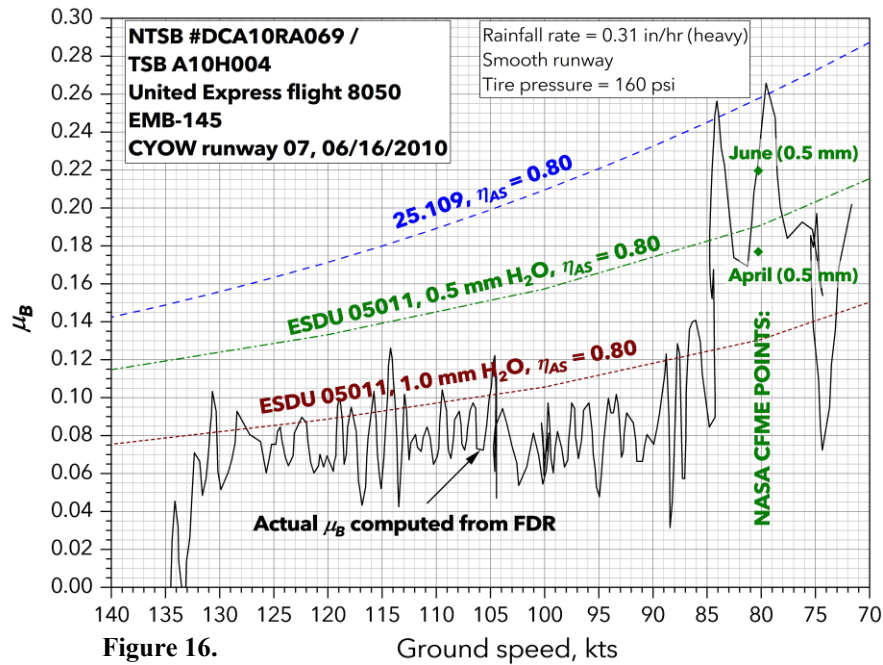


Figure 16.

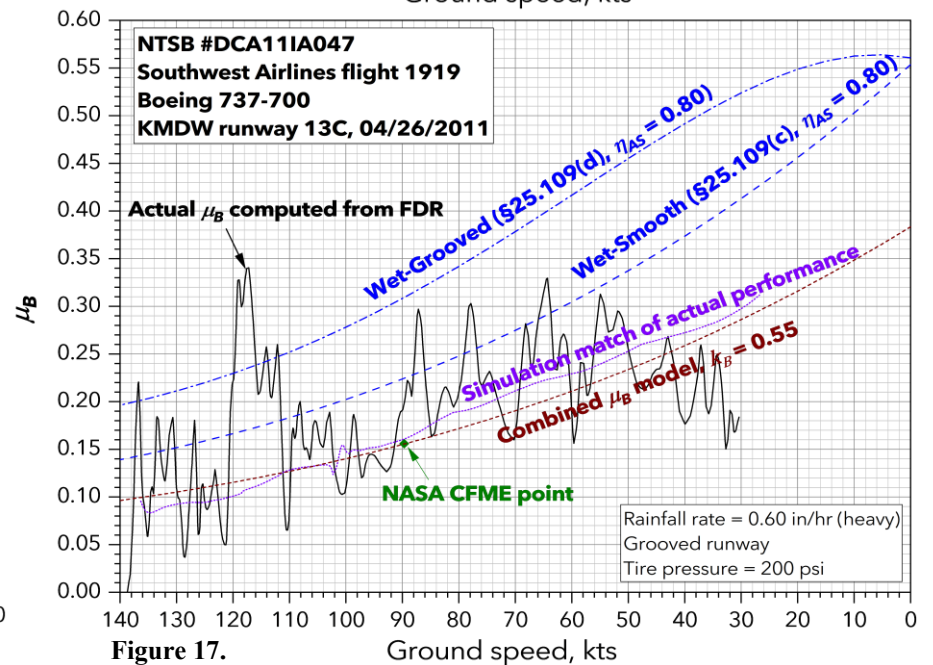


Figure 17.

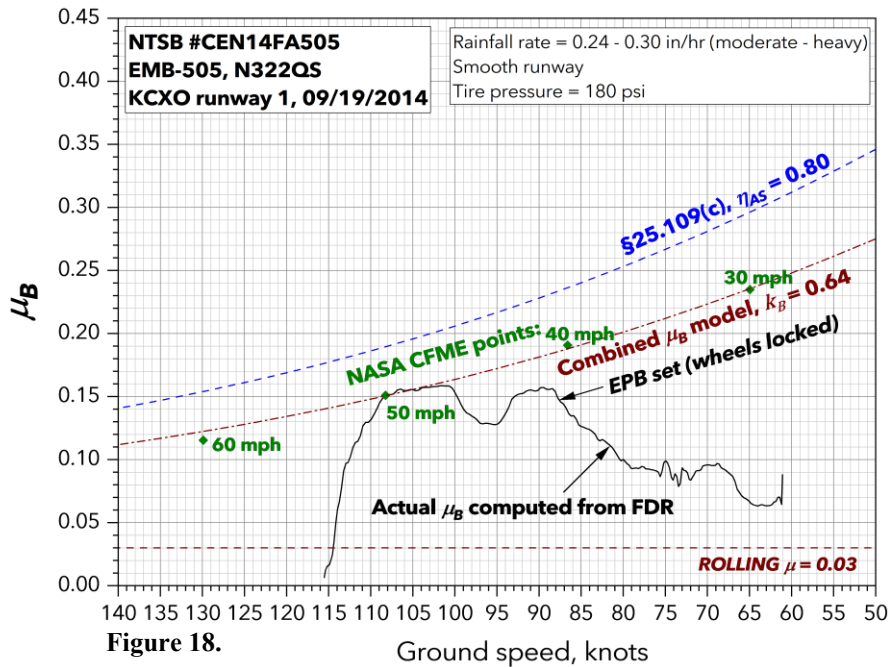


Figure 18.

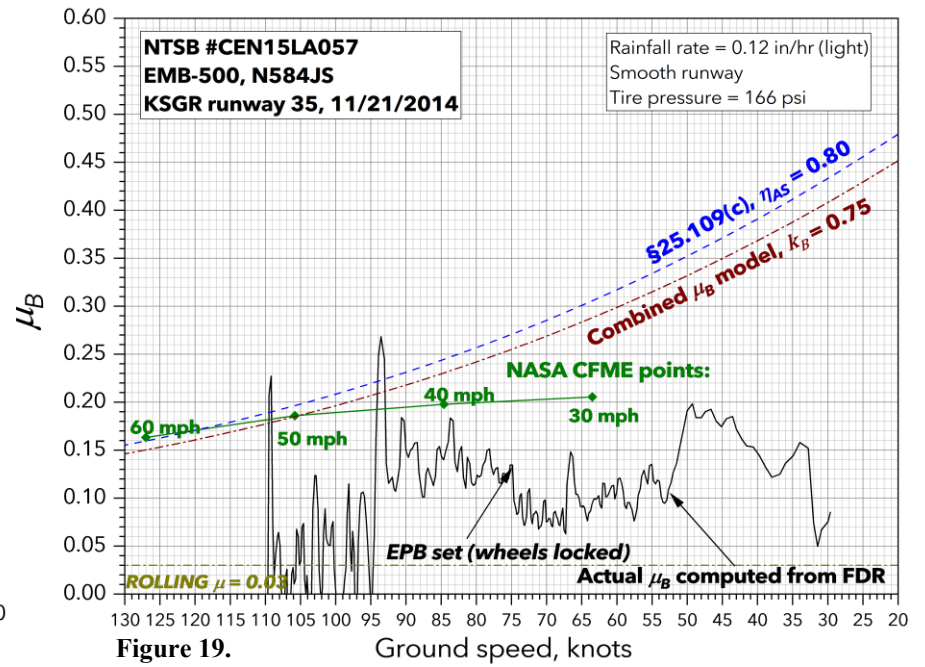


Figure 19.

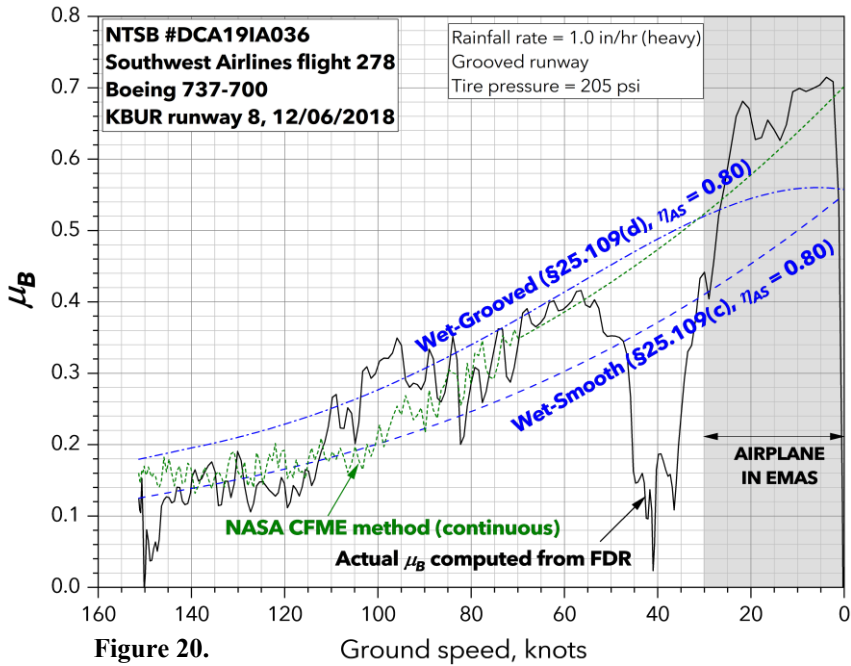


Figure 20.

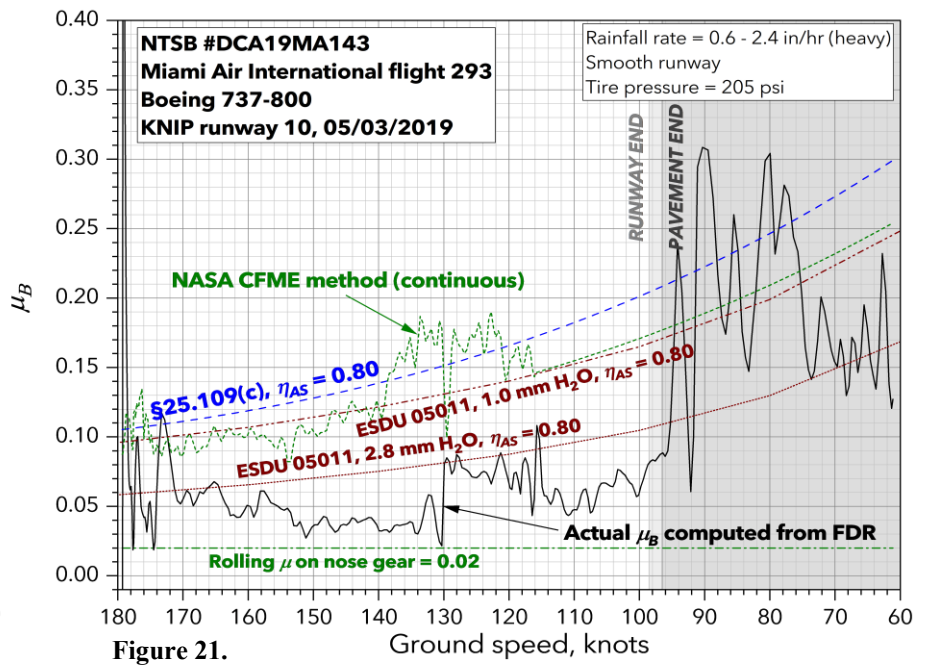


Figure 21.



Fig. 17 (Chicago) includes a line labeled “simulation match of actual performance.” This line depicts the  $\mu_B$  vs.  $V_G$  model used by Boeing to produce a simulator match of the event airplane’s performance, as recorded on the FDR. Note that the combined CFME / §25.109(c)  $\mu_B$  model (based on the average  $\mu$  obtained in a 40 mph CFME test) matches this simulation  $\mu_B$ , and the  $\mu_B$  computed from the FDR data, quite well. The §25.109(c)  $\mu_B$  overestimates the actual  $\mu_B$ , even on this grooved runway.

In the Conroe (Fig. 18) and Sugar Land (Fig. 19) events, the pilots engaged the emergency parking brake (EPB) during the landing roll, resulting in locked wheel skids and reverted rubber hydroplaning. Consequently, the  $\mu_B$  models described in this paper are not relevant after the points where the EPB was engaged. Nonetheless, Fig. 18 indicates that the CFME model matches the achieved  $\mu_B$  levels prior to the EPB engagement, and Fig. 19 indicates that the additional CFME test at 30 mph “corrects” the high  $\mu_B$  at lower speeds predicted by the “average” 50 mph test.

Figs. 16 (Ottawa) and 21 (Jacksonville) depict additional  $\mu_B$  lines labeled “ESDU 05011.” These are the results of combining the CFME and ESDU 05011 models, as described further below.

### **Estimating the ESDU 05011 F1 value from CFME data**

As described above, the ESDU 05011  $\mu_B$  model accounts for runway microtexture in a parameter called “F1,” but work to correlate values of F1 with microtexture measurements (from a laser scanner, for example) is ongoing. In the meantime, for a given runway the value of F1 can be determined such that the ESDU 05011 and the NASA CFME  $\mu_B$  models yield consistent results at the water depth corresponding to the CFME tests. The ESDU 05011 model can then be used to estimate the effect of different water depths on  $\mu_B$  at the determined value of F1. The results of using this method to estimate  $\mu_B$  at different water depths on the Ottawa and Jacksonville runways are presented in Figs. 16 and 21.

Fig. 16 shows the NASA CFME  $\mu_B$  points resulting from CFME tests conducted in April and June, 2010 (the average CFME  $\mu$  over the runway during each test was used to compute these points). In these tests, the CFME device was run with 0.5 mm of water applied in front of the measuring tire, as opposed to the 1 mm specified by the FAA for CFME measurements in the U.S.A., and as recommended by ICAO. Ref. 12 notes that

The results of [post-accident] coefficient-of-friction testing conducted from April to August 2011 indicate that, when using 0.5 mm, the friction values are above the specified [Transport Canada (TC)] guidelines for programming corrective action. However, when using 1.0 mm, the friction values are below those specified in ICAO Airport Services Manual (DOC 9137) Part 2, and immediate corrective action would have to be taken. The investigation was unable to determine the reason for the differences in published minimum friction values and testing methodology between TC and ICAO/FAA .... This difference may result in reduced runway friction levels at Canadian airports.

Consequently, it is likely that if the CFME device had been run with 1 mm of water during the April and June 2010 tests, lower  $\mu$  readings would have been obtained.

The line in Fig. 16 labeled “ESDU 05011, 0.5 mm H<sub>2</sub>O,  $\eta_{AS} = 0.8$ ” is the ESDU 05011  $\mu_B$  obtained with water depth = 0.5 mm, F1 = 3.0 (very smooth microtexture), and  $\eta_{AS} = 0.8$ . The value of F1 was selected so that the resulting  $\mu_B$  passes in-between the April and June NASA CFME  $\mu_B$  points, which were also obtained with a test tire water depth of 0.5 mm. The line labeled “ESDU 05011, 1.0 mm H<sub>2</sub>O,  $\eta_{AS} = 0.8$ ” is the ESDU 05011  $\mu_B$  obtained with water depth = 1.0 mm, F1 = 3.0, and  $\eta_{AS} = 0.8$ , and shows that, as expected, the  $\mu_B$  decreases when the water depth increases, and better matches the actual  $\mu_B$  computed from the FDR data.

For the Jacksonville case, Fig. 21 depicts the effect on  $\mu_B$  of increasing the water depth from 1.0 mm to 2.8 mm (just under the 3 mm at which the runway is considered “flooded”). The line labeled “ESDU 05011, 1.0 mm H<sub>2</sub>O,  $\eta_{AS} = 0.8$ ” is the ESDU 05011  $\mu_B$  obtained with water depth = 1.0 mm, F1 = 0.6, and  $\eta_{AS} = 0.8$ . The value of F1 was selected so that the resulting  $\mu_B$  approximately matches the “NASA CFME method (continuous)” line, which is based on a CFME run with a test tire water depth of 1.0 mm. The line labeled “ESDU 05011, 2.8 mm H<sub>2</sub>O,  $\eta_{AS} = 0.8$ ” shows that when the water depth is increased to 2.8 mm, the resulting ESDU 05011  $\mu_B$  decreases to a level much closer to the actual  $\mu_B$  computed from the FDR data. If, instead of remaining at 0.8,  $\eta_{AS}$  also decreases as  $\mu_B$  decreases (as implied by Eqn. [14a]), then the resulting  $\mu_B$  would be even lower.

The estimated water depth on the Jacksonville runway for rainfall rates up to 2 in./hr., as computed using Eqn. [9], is shown in Fig. 22. The runway x coordinate is the distance down the runway from the displaced threshold, and the runway y coordinate is the distance across the runway from the centerline. The *Aircraft Performance Study* for this accident (Ref. 13) notes that

... the lateral span of the [Boeing 737] main gear (from strut to strut) is 18.75 ft., so if the airplane tracks the centerline of the runway, both main gears should be within 10 ft. of the centerline. [Fig. 22] indicates that within this distance of the centerline, at a rainfall rate of 2 in./hr. the maximum water depth would be about 0.042” over the asphalt portion of the runway, and about 0.085” over the concrete portion of the runway. These values are within the “Safe” and “Caution” hydroplaning risk zones identified by W.B. Horne in [Ref. 14]. However, ... the airplane deviated as far as 70 ft. to the right of the runway centerline during the ground roll, and was 60 ft. to the right of the centerline when it crossed the end of the runway. [Fig. 22] indicates that at a rainfall rate of 2 in./hr., the water depth over both the asphalt and concrete portions of the runway would be in the [Ref. 14] “hydroplaning danger zone.” Even at a rainfall rate of 1.5 in./hr., which may be more representative of the conditions immediately preceding the accident, the water depths at 60 to 80 ft. from the runway centerline would be significant. As discussed above, the tire marks on the runway indicate that the tires were in contact with the pavement, and so could not have been lifted from the surface as occurs during dynamic hydroplaning. Nonetheless, the water depth (and speed) might have been sufficient to make dynamic hydroplaning imminent, and to place the tires in the condition shown in [Fig. 10c] (where there is no dry Zone 3 under the tires, and the thin, viscous water film between the pavement and the tires in Zone 2 significantly reduces  $\mu_B$ ).

In the five minutes preceding the landing of the Jacksonville airplane, the rainfall rates recorded on the field ranged from 0.6 in. / hr. to 2.4 in. / hr. Per Fig. 22, this variation in rainfall rate can result in a significant variation in the water depth (and  $\mu_B$ ) on the runway.

**DCA19MA143: Miami Air flight 293, Boeing 737-800 N732MA, Jacksonville, FL, May 3, 2019**

**Water depth on runway, based on TTI model and measured runway texture depth and cross-slope**

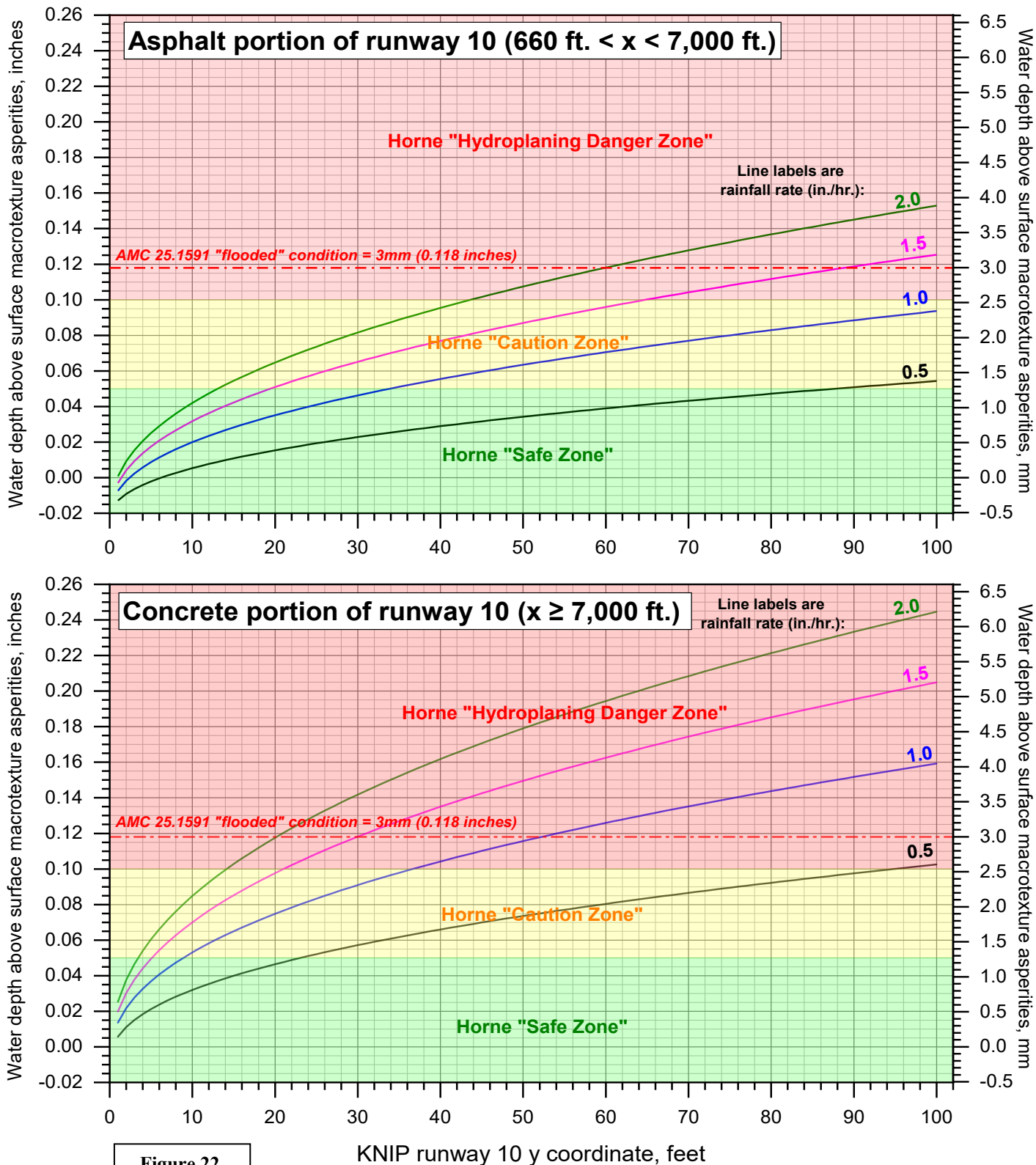


**Figure 22.**

### Guidance concerning braking performance on wet runways: SAFOs 15009 and 19003

In all of the wet-runway overruns considered above (except Burbank), the achieved  $\mu_B$  was significantly lower than the  $\mu_B$  predicted by the §25.109(c) model (corresponding to RwyCC = 5 in the RCAM), and the  $\mu_B$  required to match the manufacturers' published unfactored, wet-runway landing distances.

In recognition of the unexpectedly low  $\mu_B$  achieved in these and other events, the FAA issued SAFOs 15009 and 19003 in August 2015 and July 2019, respectively. SAFO 15009 “warns airplane operators and pilots that the advisory data for wet runway landings may not provide a safe stopping margin under all conditions,” and notes that there are typically “multiple contributing” factors to wet-runway overruns, only one of which is “less available friction than expected.” The other contributors include a long touchdown, tailwind, and “improper use of deceleration devices.”

SAFO 15009 states that “data contained in the Aircraft Flight Manuals (and/or performance supplemental materials) may underestimate the landing distance required to land on wet, ungrooved runways.” The SAFO suggests some ways of taking “appropriate action” to address the “safety concerns with landing performance on wet runways discussed in this SAFO,” such as “assuming a braking action of medium or fair when computing time-of-arrival landing performance or increasing the factor applied to the wet runway time-of-arrival landing performance data.”

SAFO 19003 “cancels and replaces SAFO 15009 and warns airplane operators and pilots that the advisory data for wet runway landings may not provide a safe stopping margin especially in conditions of Moderate or Heavy Rain.” This language is nearly identical to that in SAFO 15009, but specifies that the loss of friction might be associated with moderate or heavy rain conditions. In addition, SAFO 19003 updates the discussion in SAFO 15009 to refer to SAFO 19001 (which replaced SAFO 06012) and address the TALPA RCAM framework, and focuses on the risk of heavy rain events transitioning runways from a “wet” condition to a flooded (“contaminated”) condition:

These [landing] incidents/accidents occurred on both grooved and un-grooved runways. The data indicates that applying a 15% safety margin to wet runway time-of-arrival advisory data, as recommended by SAFO 19001 (or current guidance), may be inadequate in certain wet runway conditions. Takeoff and Landing Performance Assessment (TALPA) procedures implemented by the FAA on October 1, 2016, added new insight as to how flightcrews can evaluate runway braking performance prior to landing. TALPA defines WET as “includes damp and 1/8-inch depth or less of water,” while CONTAMINATED is “greater than 1/8-inch of water.”

**Discussion:** These overruns have occurred on grooved and smooth runways during periods of moderate to heavy rain. Analysis of these incidents/accidents indicates that the braking coefficient of friction in each case was significantly lower than expected, and that 30 to 40 percent of additional stopping distance may be required if the runway transitions from wet to contaminated based on the rainfall intensity or reported water contamination (greater than 1/8-inch depth). For the operational in-flight landing assessment, determining whether the runway is wet or potentially contaminated is the pilot's responsibility.

In the Jacksonville accident, it is likely that portions of the runway “transition[ed] from wet to contaminated based on the rainfall intensity” present shortly before the landing, consistent with the scenario described in SAFO 19003.

SAFO 19003 continues:

The FAA recommends that airports report “Wet” conditions. However, airports are not required to report when a runway is only wet. Further, an airport may not be able to generate a Field Condition NOTAM (FICON) for sudden rain showers that result in water on the runway more than 1/8 of an inch in depth (contaminated). Rainfall intensity may be the only indication available to the pilot that the water depth present on the runway may be excessive. The 1/8-inch threshold that separates a wet runway with a RWYCC of 5 from runway contaminated with water depth greater than 1/8-inch a RWYCC of 2 is based on possibility of dynamic hydroplaning. This can be especially true in moderate rain if the runway is not properly crowned, grooved, constructed with a porous friction course (PFC) overlay, or when water run-off becomes overwhelmed. During heavy rain events, this may be true even on a properly maintained grooved or PFC runway.

The TALPA RCAM recommends using landing performance data associated with medium to poor braking or RwyCC of 2, if greater than 1/8-inch of water is anticipated to be on the runway. When planning to land on a smooth runway under conditions of moderate or heavy rain, or when landing on a grooved or PFC runway under heavy rain, pilots should consider that the surface may be contaminated with water at depth greater than 1/8 inch and adjust their landing distance assessment accordingly. Pilots should use all available resources to determine what condition they may expect upon landing to include Air Traffic Control (ATC), FICONs (as some airports do report Wet conditions), flight visibility, and/or onboard weather radar.

**Note:** A Special Weather Observation (SPECI) will only be generated if a Thunderstorm begins. A SPECI is not generated when rainfall rates simply change.

Knowing ahead of time whether your aircraft can or cannot stop within the Landing Distance Available if runway conditions deteriorate to a medium to poor condition (RwyCC = 2) is critical when operating in moderate or heavy rain. Go-around, holding, or diversion may be necessary if rainfall intensity increases beyond what might be acceptable for the intended operation.

...

Unless the pilot or operator is knowledgeable of the runway’s maintenance program, and that the runway is grooved or is a PFC surface that can provide good runway friction during periods of active moderate or heavy rain, they should consider basing their time-of-arrival assessment on the above recommendations. Aircraft operators should also clarify their reporting needs to the airport operator as it relates to “Wet” runway conditions.

Significantly, SAFO 19003 notes that pilots cannot rely on the airport to know of and / or inform them of flooded (standing water) conditions resulting from heavy rainfall, and it is the rainfall intensity itself that “may be the only indication available to the pilot that the water depth present on the runway may be excessive.” Hence, the pilot’s observation of heavy rain and recognition of its potential effect on braking performance is the last line of defense against sudden flooded conditions that can defeat the landing distance safety factors required by dispatch regulations and the operator’s Flight Operations Manual. As will be discussed further below, additional rainfall rate descriptors that identify and distinguish rainfall intensities above the 0.3 in. / hr. “heavy” rain threshold could help pilots identify the potential for flooded conditions.

## Flight Test Harmonization Working Group wet runway regulatory recommendations

As indicated by SAFOs 15009 and 19003, the FAA has recognized that the actual  $\mu_B$  achieved on some wet runways may be less than that specified in §25.109(c), and that the runway length required to stop on these runways might exceed the lengths specified in AFMs. On March 8, 2013, the FAA assigned an additional task addressing wet runway stopping performance to the Transport Airplane Performance and Handling Characteristics Aviation Rulemaking Advisory Committee (ARAC). The notice in the *Federal Register* announcing this assignment (Ref. 17) states:

The FAA tasked ARAC to consider several areas within the airplane performance and handling qualities requirements of the 14 CFR part 25 airworthiness standards and guidance for possible revision. The task includes prioritizing the list of topic areas provided in this notice based on prioritization criteria established by the [Flight Test Harmonization Working Group (FTHWG)].

... The following subject areas should be considered:

...

b. Wet runway stopping performance. Recent landing overruns on wet runways have raised questions regarding current wet runway stopping performance requirements and methods. Analyses indicate that the braking coefficient of friction in each case was significantly lower than expected for a wet runway (i.e., lower than the level specified in FAA regulations). Consideration should also be given to the scheduling of landing performance on wet porous friction course and grooved runway surfaces. Recommendations may include the need for additional data gathering, analysis, and possible rulemaking.

The FTHWG started its review of wet runway stopping performance and associated  $\mu_B$  models in September, 2015. In March 2018, the FTHWG published its final report on this topic, titled *FAA Aviation Rulemaking Advisory Committee FTHWG Task 9: Wet Runway Stopping Performance Final Report: Recommendation Report, March 16, 2018* (Ref. 15). The report recommends the creation of a new 14 CFR Part 25 transport airplane certification requirement (§25.126) to determine landing distances on wet runways, to supplement the existing requirement to determine landing distances on dry runways (§25.125). In addition, the report proposes modifying the 14 CFR 121.195 operating rule to account for the wet runway landing distances required by the new §25.126 rule when dispatching airplanes to runways forecast to be wet at the time of arrival.

In general, the wet landing distances required by the recommended new §25.126 rule would have to be determined by calculation, assuming the  $\mu_B$  defined by §25.109(c), and incorporate a 10% safety margin (see Ref. 15 for details about exceptions to this requirement, such as the use of  $\mu_B$  values determined by flight test). In addition, reverse thrust could be used when determining the wet-runway landing distances (in contrast to the dry-runway landing distances required by §25.125, which must be determined without the use of reverse thrust).

The recommended change to the §121.195 operating rule would require that to dispatch a flight to a runway forecast to be wet at the time of arrival, the landing distance available must be at least 115% of the wet-runway landing distance determined per the recommended new §25.126 rule. Hence, the landing distance required at dispatch to a wet runway would be equal to the unfactored landing distance determined using the  $\mu_B$  defined by §25.109(c) and including the effect of reverse

thrust, multiplied by a total safety factor of  $1.1 \times 1.15 = 1.265$ . (The 1.1 factor is from the recommended new §25.126 rule, and the 1.15 factor is from the recommended change to §121.195.)

The FAA Transport Airplane Performance and Handling Characteristics ARAC accepted the FTHWG recommendation report in June 2018, and the proposed regulations are currently working their way through the rulemaking process.

### Rainfall rate descriptors in surface weather observations and reports

As stated above, a pilot's observation of heavy rain and recognition of its potential effect on braking performance is the last line of defense against sudden flooded conditions that can result in a required landing distance that is much longer than anticipated. Flight crews could be better prepared to anticipate flooded conditions and corresponding longer landing distances if the rain intensity descriptors provided in surface weather observations and reports (and transmitted to crews) were more granular and capable of communicating the full range of possible rainfall intensities.

The rainfall rate descriptors used in surface weather observations and reports in the U.S.A. are defined in the *Federal Meteorological Handbook No. 1: Surface Weather Observations and Reports* published by the National Oceanic and Atmospheric Administration (NOAA) (Ref. 16). The relevant tables are duplicated here as Tables 3 and 4:

Intensity	Criteria
Light	Up to 0.10 inch per hour; maximum 0.01 inch in 6 minutes.
Moderate	0.11 inch to 0.30 inch per hour; more than 0.01 inch to 0.03 inch in 6 minutes.
Heavy	More than 0.30 inch per hour; more than 0.03 inch in 6 minutes.

**Table 3.** Intensity of rain or ice pellets based on rate-of-fall (table 8-1 in Ref. 16).

Intensity	Criteria
Light	From scattered drops that, regardless of duration, do not completely wet an exposed surface up to a condition where individual drops are easily seen.
Moderate	Individual drops are not clearly identifiable; spray is observable just above pavements and other hard surfaces.
Heavy	Rain seemingly falls in sheets; individual drops are not identifiable; heavy spray to height of several inches is observed over hard surfaces.

**Table 4.** Estimating intensity of rain (table 8-2 in Ref. 16).

Note in Table 3 that “heavy” rain, the most intense rainfall rate descriptor available, corresponds to rainfall rates greater than 0.3 in./hr. The actual rainfall rates around the time of the Jacksonville accident were 2 to 8 times this threshold. The available precipitation descriptors fail to describe the significant difference between a rainfall rate of 2.4 in./hr. (8 times the “heavy” rain threshold) and 0.3 in./hr. (the threshold itself). As depicted in Fig. 22, the water depth on a runway (and the consequent  $\mu_B$ , per Fig. 21) can vary considerably over this range of rainfall rate. Consequently, a report of “heavy” rain might not communicate to flight crews the true intensity of the rainfall at

the airport, thereby impairing their ability to make a sound assessment of the runway conditions (e.g., “wet” vs. “flooded”), and the required landing distance.

Conceivably, if a broader range of potential rainfall rates can be identified using additional rainfall intensity descriptors (such as “heavy +” or “heavy ++”), then the RCAM could be updated to assign lower RwyCCs when the rainfall intensity at an airport exceeds certain thresholds, as illustrated in Table 5:

Rainfall intensity (rate) ( $I$ ), in./hr.	Descriptor	RwyCC
$0 < I \leq 0.1$	Light	5
$0.1 < I \leq 0.3$	Moderate	4
$0.3 < I \leq 0.5$	Heavy	3
$0.5 < I \leq 0.9$	Heavy +	2
$0.9 < I \leq 1.3$	Heavy ++	2
$1.3 < I$	Heavy +++	1

**Table 5.** Example possible modification of the RCAM to account for additional rainfall rate descriptors and corresponding decreased  $\mu_B$ .

In practice, the rainfall intensity descriptor thresholds and the RwyCCs corresponding to each rainfall descriptor in Table 5 would have to be determined by analysis, using methods that could include the models of water depth and corresponding  $\mu_B$  levels described previously.

As noted above, at a given rainfall intensity  $I$ , runway grooving results in additional water drainage paths and decreased water depth above the runway surface asperities. Runway grooving could be accounted for in the modified RCAM contemplated in Table 5 by decrementing the rainfall intensity used in the table:

$$I_{grooved} = I - \Delta I_{grooved} \quad [16]$$

Where  $I$  is the actual rainfall intensity,  $I_{grooved}$  is the rainfall intensity used in the modified RCAM, and  $\Delta I_{grooved}$  is the rainfall intensity decrement due to runway grooving. Again, appropriate values of  $\Delta I_{grooved}$  would have to be determined by analysis; these values might have to be functions of the actual rainfall intensity itself.

## Summary and conclusions

The wet-runway landing overrun events considered in this paper indicate that the RwyCC = 5 assigned in the RCAM to wet runways, and the corresponding  $\mu_B$  defined by §25.109(c), is insufficiently conservative. In all the events (except Burbank), the achieved  $\mu_B$  computed from FDR data is significantly below the  $\mu_B$  defined by §25.109(c). Moreover, in most cases (including Burbank), the achieved  $\mu_B$  is most consistent with the  $\mu_B$  predicted by the NASA CFME model.

The Jacksonville case indicates that when the rainfall intensity increases to the point that the water depth on the runway is well above the 1 mm used in CFME tests, the CFME model also



overestimates the achieved  $\mu_B$ . However, the CFME and ESDU 05011 models can be used together to estimate the  $\mu_B$  on a given runway at different water depths (and associated rainfall intensities). The CFME  $\mu_B$  can be used to determine the value of the microtexture sharpness parameter (F1) in the ESDU 05011 model at a water depth of 1 mm, and then this F1 value can be used in the ESDU 05011 model to determine  $\mu_B$  at other water depths.

The overrun events considered in this paper also underscore the recommendation in SAFO 19003 that

Directors of Safety and Directors of Operations (Part 121); Directors of Operations (parts 135, and 125), Program Managers, (Part 91K), and Pilots (Part 91) should ensure pilots verify, prior to initiating an approach, that the aircraft can stop within the Landing Distance Available using a RwyCC of “2” whenever there is the likelihood of moderate or greater rain on a smooth runway or heavy rain on a grooved/PFC runway.

The events also highlight that unless the language or intent of SAFO 19003 is incorporated into operators’ Operations Specifications and Flight Operations Manuals, flight crews are likely to use a RwyCC of “5” (corresponding to a wet runway), instead of “2” (corresponding to a flooded runway), when performing en-route landing distance assessments “whenever there is the likelihood of moderate or greater rain on a smooth runway or heavy rain on a grooved/PFC runway” (unless braking action reports from other flight crews change this assessment).

The weather observations surrounding the time of the Jacksonville accident all reported the precipitation condition as “heavy” rain, the most intense rainfall rate descriptor available, corresponding to rainfall rates greater than 0.3 in./hr. The actual rainfall rates around the time of the accident were 2 to 8 times the 0.3 in./hr. “heavy” rain threshold. The available precipitation descriptors fail to describe the significant difference between a rainfall rate of 2.4 in./hr. (8 times the “heavy” rain threshold) and 0.3 in./hr. (the threshold itself). Since the water depth on a runway (and the consequent  $\mu_B$ ) can vary considerably over this range of rainfall rate, a report of “heavy” rain might not communicate to flight crews the true intensity of the rainfall at the airport, thereby impairing their ability to make a sound assessment of the runway conditions (e.g., “wet” vs. “flooded”), and the required landing distance.

Conceivably, if a broader range of potential rainfall rates can be identified using additional rainfall intensity descriptors (such as “heavy +” or “heavy ++”), then the RCAM could be updated to assign lower RwyCCs when the rainfall intensity at an airport exceeds certain thresholds. Runway grooving could be accounted for in such a modified RCAM by decrementing the rainfall intensity used in the RCAM from the true rainfall intensity by a prescribed amount.

The FAA has recognized and addressed the reality of the  $\mu_B$  deficit on wet runways in several documents and actions, including SAFO 19003. Notably, the Transport Airplane Performance and Handling Characteristics ARAC has accepted recommendations from the FTHWG for new 14 CFR Part 25 and Part 121 rules to help cover, at the time of dispatch, for potentially lower-than-expected wet runway  $\mu_B$  at the destination. The overrun events discussed in this paper indicate that

the recommended rules have merit – and not just for Part 121 operators, but operators of all turbine airplanes. Hopefully, these regulations will eventually be implemented.

## Acknowledgements

The author thanks the many people who assisted in the creation and review of this paper. In particular, he thanks Tom Yager, Distinguished Research Associate at the NASA Langley Research Center (retired), for introducing him to the NASA CFME  $\mu_B$  model, and for his assistance during the KOWA investigation. The author is also grateful to Paul Giesman at the FAA Transport Standards Office (retired), for allowing him to observe the deliberations of the FTHWG, for alerting him to the need for more granular rainfall rate descriptors, and for his extensive review of Ref. 13. Many thanks also to Eric Emery at the NTSB for the statistical analysis summarized in Table 1.

## References

1. O'Callaghan, John J., *Slippery When Wet: The Case for More Conservative Wet Runway Braking Coefficient Models*. Presented at the 16<sup>th</sup> American Institute of Aeronautics and Astronautics Aviation Technology, Integration, and Operations Conference, Washington, D.C., June 17, 2016. Paper # AIAA-2016-4364, available at <https://goo.gl/rWfoUc>.
2. Engineering Science Data Unit (ESDU) Item 71025, *Frictional and Retarding Forces on Aircraft Tyres, Part I: Introduction*, issued October 1971. Sponsored by the Royal Aeronautical Society. For ESDU items see [www.esdu.com](http://www.esdu.com).
3. Engineering Science Data Unit (ESDU) Item 71026, *Frictional and Retarding Forces on Aircraft Tyres, Part II: estimation of braking force (friction data updated – 1981)*, with Amendments A and B, August 1981. Sponsored by the Royal Aeronautical Society. For ESDU items see [www.esdu.com](http://www.esdu.com).
4. National Transportation Safety Board, Office of Research and Engineering, *Group Chairman's Aircraft Performance Study, Embraer EMB-505, N322QS, Conroe, TX (Lone Star Executive Airport (KCXO)), September 19, 2014*, NTSB Accident Number CEN14FA505 (Washington, DC: NTSB, April 20, 2016). (Available through the NTSB CAROL search tool at <https://data.nts.gov/carol-main-public>).
5. NTSB letter to FAA transmitting comments on draft Advisory Circulars 25-31 and 25-32, March 4, 2015. (Available by searching the NTSB CAROL search tool at <https://data.nts.gov/carol-main-public> for recommendation A-07-057).
6. National Transportation Safety Board, Office of Research and Engineering, *Group Chairman's Aircraft Performance Study Addendum #1 (Errata #2), Hawker Beechcraft BAe 125-800A, registration N818MV, Owatonna, MN, July 31, 2008*, NTSB Accident Number DCA08MA085 (Washington, DC: NTSB, February 25, 2011). (Available through the NTSB CAROL search tool at <https://data.nts.gov/carol-main-public>).
7. Yager, Thomas J., Vogler, William A., & Baldasare, Paul, *Evaluation of Two Transport Aircraft and Several Ground Test Vehicle Friction Measurements Obtained for Various Runway Surface Types and Conditions: A Summary of Test Results From Joint FAA / NASA Runway Friction Program*. NASA Technical Paper 2917, NASA Office of Management, Scientific and Technical Information Division, February 1990.
8. B. Gallaway, R. Schiller, Jr., and J. Rose, *The Effects of Rainfall Intensity, Pavement Cross Slope, Surface Texture, and Drainage Length on Pavement Water Depths*. Texas Transportation Institute (TTI) Research Report 138-5, May 1971.

9. Engineering Science Data Unit (ESDU) Item 10015, *Model for performance of a single aircraft tyre rolling or braking on dry and precipitate contaminated runways, Amendment (C)*, released April 2023. For ESDU items see [www.esdu.com](http://www.esdu.com).
10. Engineering Science Data Unit (ESDU) Item 05011, *Aircraft tyre rolling or braking on dry or precipitate contaminated runways: Summary of the model, Amendment (E)*, released April 2023. For ESDU items see [www.esdu.com](http://www.esdu.com).
11. Van Es, Gerard, *How to assess runway micro texture in overruns on wet runways?* Paper presented at the ISASI 2021 Annual Seminar, Aug 30- Sept 2, 2021.
12. Transportation Safety Board of Canada, *Aviation Investigation Report A10H0004: Runway Overrun, Trans States Airlines LLC, Embraer EMB-145LR N847HK, Ottawa / Macdonald-Cartier International Airport, Ontario, 16 June 2010*, available at: <http://www.tsb.gc.ca/eng/rappports-reports/aviation/2010/A10H0004/A10H0004.asp>.
13. National Transportation Safety Board, Office of Research and Engineering, *Group Chairman's Aircraft Performance Study, Miami Air International flight 293, Boeing 737-81Q, N732MA, Jacksonville, FL (Jacksonville Naval Air Station (KNIP)), May 3, 2019*, NTSB Accident Number DCA19MA143 (Washington, DC: NTSB, April 9, 2021). (Available through the NTSB CAROL search tool at <https://data.nts.gov/carol-main-public>).
14. Horne, Walter B. *Wet Runways*, NASA Technical Memorandum TM-X-72650, NASA Langley Research Center, Hampton, VA, April 1975. Available at <https://ntrs.nasa.gov/archive/nasa/casi.ntrs.nasa.gov/19750012279.pdf>.
15. Federal Aviation Administration (FAA) Aviation Rulemaking Advisory Committee (ARAC) Flight Test Harmonization Working Group (FTHWG), Task 9: *Wet Runway Stopping Performance Final Report, Recommendation Report, March 16, 2018*. Available at: [https://www.faa.gov/regulations\\_policies/rulemaking/committees/documents/media/FTHWG-%20Wet%20Runway%20Topic9%20Final%20Report.pdf](https://www.faa.gov/regulations_policies/rulemaking/committees/documents/media/FTHWG-%20Wet%20Runway%20Topic9%20Final%20Report.pdf).
16. U.S. Department of Commerce / National Oceanic and Atmospheric Administration (NOAA), Office of the Federal Coordinator for Meteorological Services and Supporting Research (OFCM), *Federal Meteorological Handbook No. 1: Surface Weather Observations and Reports*, document FCM-H1-2019, Washington, D.C., July 2019. Available at [https://www.ofcm.gov/publications/fmh/FMH1/fmh1\\_2019.pdf](https://www.ofcm.gov/publications/fmh/FMH1/fmh1_2019.pdf).
17. *Federal Register* Vol. 78, No. 46 / Friday, March 8, 2013 / Notices, page 15112.
18. Wray, Gilbert A., *A Systematic Experimental Investigation of Significant Parameters Affecting Model Tire Hydroplaning*, NASA CR-132346, Davidson Laboratory Report SIT-DL-72-1602, July 1973. Available at: <https://ntrs.nasa.gov/archive/nasa/casi.ntrs.nasa.gov/19740003931.pdf>.

## Glossary

### Acronyms

AC	Advisory Circular
AFM	Airplane Flight Manual
ARAC	Aviation Rulemaking Advisory Committee
ATC	Air Traffic Control
CFME	Continuous Friction Measurement Equipment
CFR	Code of Federal Regulations
CYOW	Ottawa Macdonald-Cartier International Airport, Ottawa, Ontario
EASA	European Aviation Safety Agency
EPB	Emergency parking brake
ESDU	Engineering Science Data Unit

FAA	Federal Aviation Administration
FCOM	Flight Crew Operating Manual
FDR	Flight Data Recorder
KBUR	Bob Hope Airport, Burbank, California
KCXO	Lone Star Executive Airport, Conroe, Texas
KMDW	Chicago Midway International Airport, Chicago, Illinois
KNIP	Jacksonville Naval Air Station, Jacksonville, Florida
KOWA	Owatonna Degner Regional Airport, Owatonna, Minnesota
KSGR	Sugar Land Regional Airport, Sugar Land, Texas
METAR	Meteorological Terminal Air Report
MKJP	Norman Manley International Airport, Kingston, Jamaica
NASA	National Aeronautics and Space Administration
NTSB	National Transportation Safety Board
RCAM	Runway Condition Assessment Matrix
RwyCC	RCAM runway condition code
SAFO	Safety Alert For Operators
SPECI	Special meteorological report or forecast
TALPA	Takeoff And Landing Performance Assessment
TTI	Texas Transportation Institute
U.S.A.	United States of America

*English symbols*

$d$	Average water depth above the top of the runway macrotexture
$F_N$	Longitudinal reaction force at nose gear
$F_M$	Longitudinal reaction force at main gear
$F_x$	Force along body x-axis
$F_z$	Force along body z-axis
$g$	Gravitational acceleration
$I$	Rainfall intensity
$k_B$	Effective $\eta_{AS}$ for scaling §25.109(c) $\mu_{max}$ to $\mu_B$ from CFME runs
$L$	Runway drainage path-length (distance from runway centerline)
$M_y$	Moment about body y-axis
$n_x$	Longitudinal load factor
$n_y$	Lateral load factor
$N1$	Engine fan speed
$N_N$	Vertical reaction force at nose gear
$N_M$	Vertical reaction force at main gear
$p$	Tire pressure
$r_{TIRE}$	Effective tire radius
$s$	Wheel slip ratio
$s_{\mu,MAX}$	Wheel slip ratio for $\mu_{B,MAX}$
$S$	Runway cross slope

$T$	Runway macrotexture depth
$V_G$	Airplane ground speed
$V_1$	Takeoff decision speed
$V_p$	Hydroplaning speed (for dynamic hydroplaning)
$V_{p,spin\ down}$	Spin-down hydroplaning speed (rotating tire)
$V_{p,spin\ up}$	Spin-up hydroplaning speed (nonrotating tire)
$V_{WHEEL}$	Tangential speed of tire
$W$	Airplane weight
$W_x$	Component of airplane weight along body x-axis
$W_y$	Component of airplane weight along body y-axis
$W_z$	Component of airplane weight along body z-axis
$x$	Runway x coordinate
$y$	Runway y coordinate

### Greek symbols

$\alpha$	Angle of attack
$\gamma$	Flight path angle / runway slope
$\eta_{AS}$	Anti-skid braking system efficiency
$\theta$	Pitch angle
$\mu$	Friction coefficient
$\mu_B$	Wheel braking friction coefficient
$\mu_{B,MAX}$	Maximum wheel braking friction coefficient (at $s_{\mu,MAX}$ )
$\mu_{B,SKID}$	Wheel braking friction coefficient with locked wheels (i.e., at $s=1$ )
$\mu_{CFME}$	Runway $\mu$ measured by a CFME device
$\mu_{dry}$	Dry-runway $\mu$
$\mu_N$	Rolling friction coefficient at nose gear
$\mu_{max}, \mu_{t/gMAX}$	Maximum $\mu$ available on runway
$\mu_{wet}$	Wet-runway $\mu$
$\omega_{WHEEL}$	Wheel angular velocity

### Endnotes

<sup>1</sup> A related but different type of accident is one in which the pilot, perceiving that the airplane will not stop on the paved surface, decides to abort a landing late in the landing roll and take off again, but the airplane fails to clear obstacles beyond the departure end of the runway. Because of the higher energy involved, these types of accidents usually result in greater injury than landing overruns. The Owatonna case considered in this paper is such an accident (see Refs. 1 and 6).

<sup>2</sup> See *A40 SkyTalks: Global Reporting System Format (GRF): Be Aware, Get Ready* on YouTube at: <https://www.youtube.com/watch?v=eBzCkX-5a3g&t=10s>.

<sup>3</sup> Precise, formal definitions of “wet” and “contaminated” are given in AC 25-32 and quoted below.

<sup>4</sup> The rolling friction coefficient is typically 0.02 to 0.03.

---

<sup>5</sup> The NTSB’s final report on this accident, including the probable cause, findings, and safety recommendations, can be found at <https://www.nts.gov/investigations/AccidentReports/Reports/AAR0706.pdf>.

<sup>6</sup> As discussed below, a subsequent Aviation Rulemaking Advisory Committee (ARAC) has in fact recommended an addition to preflight (or dispatch) landing distance requirements, to account for the shortfall in the expected runway friction observed in a number of wet runway landing overruns.

<sup>7</sup> At the same time, the FAA published *Advisory Circular AC 25-31, Takeoff Performance Data for Operations on Contaminated Runways*, containing guidance for developing takeoff performance data on contaminated runways.

<sup>8</sup> 85% of the spin-down hydroplaning speed, defined in Equation [8a], is equivalent to the spin-up hydroplaning speed, defined in Equation [8b]. AC 25-32 defines the “hydroplaning speed” as the spin-down hydroplaning speed (Equation [8a]).

<sup>9</sup> Per 14 CFR 1.2,  $V_1$  “means the maximum speed in the takeoff at which the pilot must take the first action (e.g., apply brakes, reduce thrust, deploy speed brakes) to stop the airplane within the accelerate-stop distance.  $V_1$  also means the minimum speed in the takeoff, following a failure of the critical engine at  $V_{EF}$ , at which the pilot can continue the takeoff and achieve the required height above the takeoff surface within the takeoff distance.”

<sup>10</sup>This simplified definition suffices for the intent of this paper; §25.109 defines additional details regarding how this maneuver is to be accomplished, that account for engine failures and pilot reaction times.

<sup>11</sup> See AC 25-7D, paragraph 4.3.7.4, “Classification of Types of Anti-Skid Systems.”

<sup>12</sup> 14 CFR §25.109(d) specifies 5<sup>th</sup>-order polynomials defining  $\mu_B$  as a function of  $V_G$  for a grooved or “porous friction course” runway, similar to the cubic (3<sup>rd</sup>-order) polynomials defined in §25.109(c) for a smooth runway.